Winter-spring warming in the North Atlantic during the last 2,000 years: Evidence from Southwest Iceland

Nora Richter[1, 2], James M. Russell[1], Johanna Garfinkel[1], Yongsong Huang[1]

[1] Department of Earth, Environmental and Planetary Sciences, Brown University, Providence, RI 02912, USA
[2] The Josephine Bay Paul Center for Comparative Molecular Biology and Evolution, Marine Biological Laboratory, Woods Hole, MA, 02543, USA

Correspondence to: Nora Richter (nora.richter@nioz.nl)

Abstract. Temperature reconstructions from the Northern Hemisphere (NH) generally indicate cooling over the Holocene which is often attributed to decreasing summer insolation. However, climate model simulations predict that rising atmospheric CO_2 concentrations and the collapse of the Laurentian ice sheet caused mean annual warming during this epoch. This contrast could reflect a seasonal bias in temperature proxies, and particularly a lack of proxies that record cold (late fall-early spring) season temperatures, or inaccuracies in climate model predictions of NH temperature. We reconstructed winter-spring temperatures during the Common Era (i.e. the last 2,000 years) using alkenones, lipids produced by Isochrysidales haptophyte algae that bloom during spring ice-off, preserved in sediments from Vestra Gíslholtsvatn (VGHV), southwest Iceland. Our record indicates that winter-spring ~~cold-season~~ temperatures warmed during the last 2,000 years, in contrast to most NH averages. Sensitivity tests with a lake energy balance model suggest that warmer winter and spring air temperatures result in earlier ice-off dates and warmer spring lake water temperatures, and therefore warming in our proxy record. Regional air temperatures are strongly influenced by sea surface temperatures during the winter and spring season. SSTs respond to both changes in ocean circulation and gradual changes in insolation~~and both of whichtemperatures at our study site~~. ~~Sensitivity tests with a lake energy balance model show that this warming is likely driven by increasing winter-spring insolation.~~ We also found distinct seasonal differences in centennial-scale, cold-season temperature variations in VGHV compared to existing records of summer and annual temperatures from Iceland. M~~Sustained or abrupt cooling in VGHV temperatures are associated with the cumulative effects of solar minima and volcanic eruptions, and potentially ocean and sea-ice feedbacks associated with cooling in the broader Arctic. However, m~~ulti-decadal to centennial-scale changes in winter-spring temperatures were

Formatted: Font color: Red

Formatted: Font color: Auto

Formatted: Font color: Auto

Formatted: Font color: Auto

Formatted: Font color: Auto

strongly modulated by internal climate variability and changes in regional ocean circulation~~, i.e. the North Atlantic Oscillation~~, which can result in winter and spring warming in Iceland even after a major negative radiative perturbation.

Formatted: Font color: Auto

Formatted: Font color: Auto

Formatted: Font color: Auto

1 Introduction

Temperatures in the Northern Hemisphere (NH) are generally thought to have cooled over the past 2,000 years, culminating in the Little Ice Age (LIA, c. 1450-1850 CE) (Kaufman et al., 2009; PAGES 2K Consortium, 2013, 2019; McKay and Kaufman, 2014). However, the majority of NH temperature reconstructions are based on proxies that respond to climate change during the warm season and may not capture trends in annual or winter and spring temperatures (Liu et al., 2014; PAGES 2K Consortium, 2019). This limits our understanding of major atmospheric phenomena in the NH, such as the North Atlantic Oscillation (NAO) which dominates wintertime variability, as well as changes in ocean circulation and other phenomena driving variability in the extent of Arctic sea ice.

Many oceanic and atmospheric processes that influence surface climate in the Atlantic and the broader NH are centered in the high North Atlantic region, making it an important location to study changes during the winter and spring seasons (Hurrell, 1995; Yeager and Robson, 2017). Terrestrial paleoclimate records from Iceland, for instance, have the potential to resolve temperature changes during the winter and spring seasons as this region is sensitive to the NAO and sits near the southern limit of Arctic sea ice (Hurrell, 1995; Hanna et al., 2004, 2006). The high sedimentation rates in Icelandic lakes, along with well-known volcanic eruptions that can be used as age constraints on sediment successions, make this an ideal location and archive to test how winter and spring temperatures evolved over the past 2,000 years (Larsen and Eiríksson, 2008; Geirsdóttir et al., 2009, 2019; Larsen et al., 2011; Langdon et al., 2011; Holmes et al., 2016). However, existing terrestrial records of temperature from Iceland are limited due to their sensitivity to the warm season, low temporal resolution and length, or compounding effects on proxies from human land-use or precipitation over the past 2,000 years.

Here we present a reconstruction of winter-spring temperatures developed using well-dated lake sediments from southwest Iceland to assess seasonal temperature changes in the North Atlantic climate over the past 2,000 years. We take advantage of alkenone-production by Group I Isochrysidales (i.e. haptophyte algae) during the spring season to develop a record of winter-spring temperatures and investigate the forcings responsible for cold-season temperature changes using a lake energy balance model.

2 Methods

2.1 Study site and age model

Vestra Gíslholtsvatn (VGHV) is a small lake (1.57 km^2) located in southwest Iceland (61 m a.s.l., 63° 56′ N, 20° 31′ W; Fig. 1), about 25 km from the coast (Blair et al., 2015). Mean monthly temperatures range from -1.4 °C during the winter months (DJF) to 10.4 °C during the summer months (JJA) (station at Hella, 1958-2005 CE; Icelandic Meteorological Office). Cores were collected in 2008 using a Bolivia piston coring system (Blair et al., 2015), and were sampled at the National Lacustrine Core Facility (LacCore) at the University of Minnesota.

The VGHV cores were dated using previously identified tephra, including seven historical and four pre-historical tephra beds (Blair et al., 2015 and references therein). The age model was developed using 'classical' age modeling (CLAM) with a smoothed spline fit (Blaauw, 2010). The resulting age model has an uncertainty of 5 to 15 yrs from -50 to 1200 yrs BP and 18 to 83 yrs from 1201 to 2000 yrs BP (Fig. 2; ~~Blaauw, 2010~~).

Formatted: Not Highlight

Field Code Changed

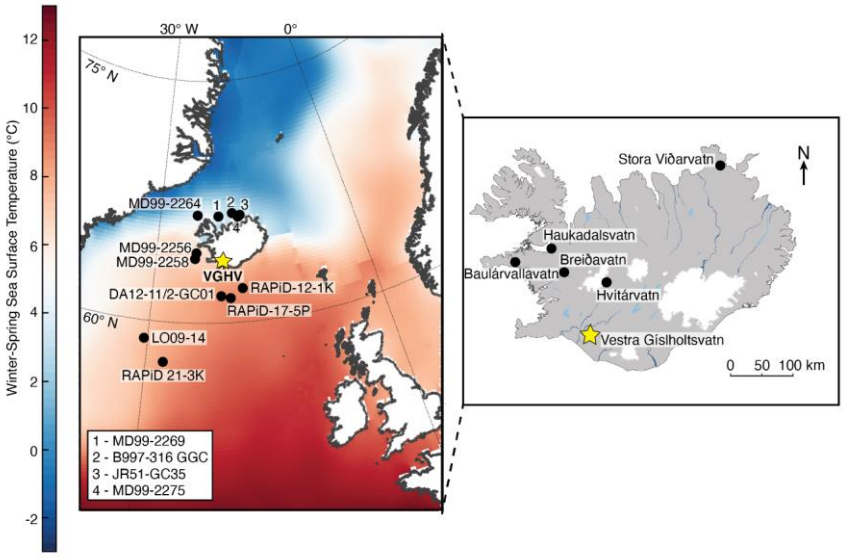

Figure 1. Map of mean winter-spring (DJFMAM) sea surface temperatures from 1955-2017 in the high North Atlantic region. The marine sediment cores MD99-2269 (Moros et al., 2006; Justwan et al., 2008; Cabedo-Sanz et al., 2016), B997-316 GGC (Harning et al., 2019), JR51-GC35 (Cabedo-Sanz et al., 2016), MD99-2275 (Jiang et al., 2005, 2015; Massé et al., 2008; Sicre et al., 2008; Ran et al., 2011), MD99-2264 (Ólafsdóttir et al., 2010), MD99-2256 (Ólafsdóttir et al., 2010), MD99-2258 (Axford et al., 2011), DA12-11/2-GC01 (Orme et al., 2018; Van Nieuwenhove et al., 2018), RAPiD-12-1K (Thornalley et al., 2009), RAPiD-17-5P (Moffa-Sánchez et al., 2014), LO09-14 (Berner et al., 2008), and RAPiD 21-3K (Sicre et al., 2011; Miettinen et al., 2012) that are discussed in the text are indicated. The ~~the~~ locations of lake sediment records from Stora Viðarvatn (Axford et al., 2009), Haukadalsvatn (Geirsdóttir et al., 2009), Baulárvallavatn (Holmes et al., 2016), Breiðavatn (Gathorne-Hardy et al., 2009), and Hvítárvatn (Larsen et al., 2011) are indicated. The study site, Vestra Gíslholtsvatn (VGHV), is marked by a yellow star. The maps were made using data from Natural

Earth, the National Land Survey of Iceland, and the National Oceanic and Atmospheric Administration (NOAA) World Ocean Database (Boyer et al., 2018).

2.2 Lipid analyses

Sediments were freeze-dried and extracted using a Dionex™ accelerated solvent extraction (ASE 350) system at 120 °C and 1200 psi. All of the extracts were separated by silica gel (40-63 µm, 60 Å) flash chromatography to obtain alkane (hexane; Hex), ketone (dichloromethane; DCM), and polar (methanol; MeOH) fractions. Saponification was used to remove wax esters by dissolving the dried ketone fraction in a 1 molar potassium hydroxide solution with MeOH:H_2O (95:5, v/v) and heating the samples for 3 hrs at 65 °C. 5 % NaCl in H_2O and 50 % HCl in H_2O were added to the samples and the lipid faction was extracted using Hex (100 %). Ketone fractions were further purified using silver nitrate columns (D'Andrea et al., 2007) with DCM (100 %) followed by ethyl acetate (100 %) to elute the alkenones. If additional cleaning was needed, a modified procedure from Salacup et al. (2019) was used. The alkenone fraction was dried under N_2 gas and re-dissolved in 1.5 mL of DCM:Hex (2:1, v/v). To this, a 1.5 mL solution of 100 mg/mL urea in MeOH was added. The resulting crystals were dried under N_2 gas, and the urea addition was repeated two more times. The dried urea crystals were cleaned with Hex (100 %) and extracted as the non-adduct. Milli-Q water was added to the vial to fully dissolve the urea crystals, and the adduct was extracted using Hex (100 %). The samples were then analyzed for alkenones. For several samples, co-eluting compounds were still present, or concentrations were too low for reliable quantification. These samples were not included in our final reconstruction.

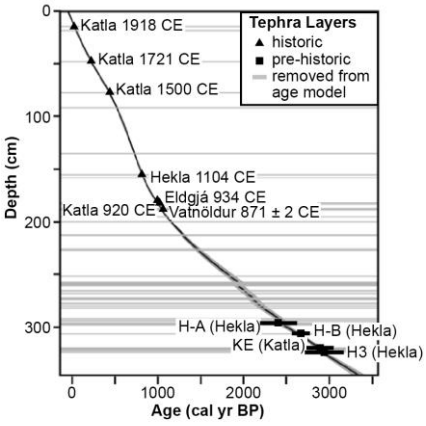

Figure 2. Age model for Vestra Gíslholtsvatn with historic and pre-historic tephra layers (previously identified by Blair et al., 2015 and Christensen, 2013) indicated (figure adapted from Richter et al., 2021).

~~**Figure 2. Age model for Vestra Gíslholtsvatn with historic and pre-historic tephra layers (previously identified by Blair et al., 2015 and references therein) used for dating indicated. The gray lines represent tephra layers that were removed from the age model.**~~

The resulting alkenone fraction was analyzed using an Agilent 6890N gas chromatography (GC) and flame ionization detector (FID) system with an Agilent VF-200ms capillary column (60 m x 250 µm x 0.10 µm). Samples were injected into a CIS-PTV inlet in solvent vent mode (6.9 psi at 112 °C). The oven program was set to 50 °C and increased to 235 °C at 20 °C/min and ramped to 320 °C at 1.39 °C/min where it was held isothermally for 5 min. An alkenone standard was injected twice every 8 to 10 samples to assess the analytical precision of the alkenone measurements. The standard deviation for the calculated U^{K}_{37} index (see equation 1) was 0.0040 (n = 28). For additional verification or identification of co-eluting compounds, samples were run on an Agilent 6890N GC system coupled with an Agilent 5793 N quadrupole mass spectrometer (MS). All samples were injected with pulsed splitless injection mode (20 psi at 315 °C) and run on an Agilent VF-200ms capillary column (60 m x 250 µm x 0.10 µm). The oven program was started at 40 °C for 1 min, ramped up to 255 °C at 20 °C/min, increased again to 315 °C at 2 °C/min, and then held isothermally for 10 min. The MS ionization energy was set to 70 eV with a scan range of 50 to 600 *m/z*.

Formatted: Font: (Default) +Headings (Times New Roman)
Formatted: Font: (Default) +Headings (Times New Roman), Font color: Auto
Formatted: Font: (Default) +Headings (Times New Roman)
Formatted: Font: (Default) +Headings (Times New Roman)
Formatted: Font: (Default) +Headings (Times New Roman)
Formatted: Font: (Default) +Headings (Times New Roman)
Formatted: Font: (Default) +Headings (Times New Roman)
Formatted: Font: (Default) +Headings (Times New Roman)
Formatted: Font: (Default) +Headings (Times New Roman), Font color: Auto
Formatted: Font color: Auto

2.3 Alkenones as a proxy for lake water temperatures

Alkenones are long-chain ketones produced by Isochrysidales haptophyte algae in both marine and lacustrine environments. Numerous marine-based culture and core-top studies show that variations in alkenone saturation (i.e., changes in $C_{37:3}$Me and $C_{37:2}$Me production) are inversely correlated with temperature, and can be linearly calibrated to temperature using either the U^{K}_{37} or $U^{K'}_{37}$ index (Brassell et al., 1986; Prahl and Wakeham, 1987; Prahl et al., 1988; Müller et al., 1998; Conte et al., 2006). Similarly, culture studies, core tops, and in situ measurements in lakes show that changes in alkenone saturation are also correlated with temperature (Zink et al., 2001; Sun et al., 2007; Toney et al., 2010; D'Andrea et al., 2011, 2012, 2016; Wang and Liu, 2013; Nakamura et al., 2014; Longo et al., 2016, 2018; Zheng et al., 2016). The U^{K}_{37} index can be applied to lacustrine environments and is calculated as follows:

$$U^{K}_{37} = \frac{[C_{37:2}Me] - [C_{37:4}Me]}{[C_{37:2}Me] + [C_{37:3}Me] + [C_{37:3*}Me] + [C_{37:4}Me]} \quad (1)$$

Sedimentary alkenones may derive from multiple alkenone-producing species, mainly Group I and II Isochrysidales, with distinct alkenone signatures and varying responses to temperature (Coolen et al., 2004; Sun et al., 2007; Theroux et al., 2010, 2013; Ono et al., 2012; Toney et al., 2012; Nakamura et al., 2014; D'Andrea et al., 2016). Group I Isochrysidales produces distinct tri-unsaturated alkenones (e.g., $C_{37:3*}$Me and $C_{38:3*}$Et), which can be used to test for species-mixing effects with the RIK_{37} and RIK_{38E} ~~i~~indices~~x~~ (Longo et al., 2016):

Formatted: Subscript

$$RIK_{37} = \frac{[C_{37:3}Me]}{[C_{37:3}Me + C_{37:3^*}Me]} \quad (2)$$

$$RIK_{38E} = \frac{[C_{38:3}Et]}{[C_{38:3}Et + C_{38:3^*}Et]} \quad (3)$$

A RIK_{37} value of 1.0 suggests a predominance of the $C_{37:3}$Me and the presence of Group II Isochrysidales, while values from 0.48 to 0.63 are empirically shown to correspond to Group I Isochrysidales (Longo et al., 2016, 2018). RIK_{38E} values of 0 to 0.57 were empirically shown to correspond to Group I alkenone distributions, whereas Group II alkenone distributions correspond to values between 0.75 to 1 (Longo et al., 2016, 2018).

Group I Isochrysidales and their corresponding alkenones have, so far, only been identified in Northern Hemisphere lakes at latitudes ranging from 42-81 °N (Longo et al., 2018; Richter et al., 2019). The Northern Hemisphere lake calibration for Group I alkenones, which includes VGHV, was developed using the average spring temperatures for each lake during ice-off and the main Group I Isochrysidales bloom (U^{K}_{37} = 0.029*T*-0.49, r^2 = 0.60, RMSE = ± 1.69°C; Longo et al., 2018). ~~An updated~~The calibration for Group I ~~that~~ was updated to include~~s~~ additional lakes in northeastern China (U^{K}_{37} = 0.030*T*-0.47~~79~~, r^2 = 0.~~0~~48~~79~~) and now has an RMSE = ± 1.71°C (Yao et al., 2019). Group I alkenone calibrations also exist for Lake BrayaSø in Greenland (U^{K}_{37} = 0.025~~45~~*T*-0.78~~79~~, r^2 = 0.96, note the calibration also includes data from several German lakes, see Zink et al., 2001; D'Andrea et al., 2011), Lake Kongressvatnet in Svalbard (U^{K}_{37} = 0.026~~55~~*T*-0.804, r^2 = 0.85, D'Andrea et al., 2012), Toolik Lake in Alaska (U^{K}_{37} = 0.021*T*-0.68, r^2 = 0.85; Longo et al., 2016), and Vikvatnet in Norway (U^{K}_{37} = 0.0284*T*-0.66~~55~~, r^2 = 0.94; D'Andrea et al., 2016).

Temperature calibrations using the U^{K}_{37} index were ~~successfully~~ applied to develop high resolution records of summer temperatures in Greenland (c. 5,600 yrs BP; D'Andrea et al., 2011) and ~~and~~ Svalbard (1,800 yrs BP; D'Andrea et al., 2012 and 12,000 yrs BP; van der Bilt et al., 2018, 2019), as well as ~~and~~ a winter-spring temperature record in Alaska (16,000 yrs BP; Longo et al., 2020). ~~However, regional variability in the relationship between the U^{K}_{37} index and temperature requires the development of local temperature calibrations (Wang and Liu, 2013; D'Andrea et al., 2016; Longo et al., 2016).~~~~Unfortunately, there is currently no local calibration for Icelandic lakes.~~

~~It is also important to note that t~~The main timing of ice-off, and the corresponding alkenone bloom in VGHV, occurs in April to May in southern Iceland and May to June in northern Iceland (see Tables A2 & A3). In contrast, studies in Svalbard report ice-off dates between late June to mid-August and show that alkenones primarily record summer (JJA) temperatures (D'Andrea et al., 2012; van der Bilt et al., 2019). I~~, whereas i~~n Northern Alaska ice-off dates primarily occur in June and reflect temperature changes during the winter and spring season (Longo et al., 2018, 2020). The regional variability in the relationship between

Formatted: Dutch (Netherlands)
Formatted: Dutch (Netherlands)
Formatted: Dutch (Netherlands)
Formatted: Dutch (Netherlands)
Formatted: Dutch (Netherlands)
Formatted: Dutch (Netherlands)
Formatted: Dutch (Netherlands)
Formatted: Dutch (Netherlands)
Formatted: Dutch (Netherlands)
Formatted: Dutch (Netherlands)
Formatted: Dutch (Netherlands)
Formatted: Dutch (Netherlands)
Formatted: Dutch (Netherlands)
Formatted: Dutch (Netherlands)
Formatted: Dutch (Netherlands)
Formatted: Dutch (Netherlands)
Formatted: Dutch (Netherlands)
Formatted: Dutch (Netherlands)
Formatted: Dutch (Netherlands)
Formatted: Dutch (Netherlands)
Formatted: Dutch (Netherlands)
Formatted: Dutch (Netherlands)
Formatted: Dutch (Netherlands)
Formatted: Dutch (Netherlands)
Formatted: Dutch (Netherlands)
Formatted: Dutch (Netherlands)
Formatted: Dutch (Netherlands)
Formatted: Dutch (Netherlands)
Formatted: Dutch (Netherlands)
Formatted: Dutch (Netherlands)
Formatted: Dutch (Netherlands)
Formatted: Subscript
Formatted: Font color: Auto
Formatted: Font color: Auto
Formatted: Font color: Auto
Formatted: Font color: Auto
Formatted: Font color: Auto
Formatted: Font color: Auto
Formatted: Font color: Auto

the U^{K}_{37} index and temperature, as well as differences in the timing of the alkenone bloom requires the development of local temperature calibrations and validation of the ~~proxy~~ seasonal~~ity~~ sensitivity of the proxy for each region (Wang and Liu, 2013; D'Andrea et al., 2016; Longo et al., 2016). Unfortunately, there is currently no local calibration for Icelandic lakes, but i~~I~~n the following section we will describe how we use a lake model to test what drives changes in ice-off dates and lake water temperatures, and therefore the seasonality of temperature recorded by alkenones, in VGHV.

~~Unfortunately, there is currently no local calibration for Icelandic lakes.~~

2.4 Seasonal temperature sensitivity of Group I alkenones in lakes

In Greenland and Alaska, Group I Isochrysidales bloom during the early spring in the photic zone as lake ice starts to melt (D'Andrea and Huang, 2005; D'Andrea et al., 2011; Longo et al., 2016, 2018). Alkenone production starts prior to ice-off, then increases as the lake undergoes isothermal mixing, and decreases when thermal stratification begins to develop in late spring/early summer (Longo et al., 2018). This holds true for other Group I-containing lakes in the NH, including lakes in Iceland, as evidenced by the positive correlation between the U^{K}_{37} index and mean spring air temperatures (Longo et al., 2018).

We investigated the controls on spring lake water temperatures and the timing of ice-melt in VGHV using a lake energy balance model (Dee et al., 2018). The purpose of the lake model was to determine the sensitivity of our proxy to different forcing mechanisms by assessing the ~~magnitude of the~~ temperature response and timing of ice-melt relative to our control simulation. Due to the lack of ~~an extensive local dataset~~extensive observational datasets from VGHV ~~by which~~ to test our model, we adjusted the initial parameters using available data in the literature and parametrizations determined by Longo et al. (2020) for lakes in Northern Alaska, where the lake model was validated using limnological data from the Toolik Environmental Data Center and the Arctic Long-Term Ecological Research program over a 6-year period (see Table A1). Lake E5 in Northern Alaska is similar in size and with a similar catchment area to VGHV (Longo et al., 2020). The neutral drag coefficient was set to 0.002, and the albedos for slush and snow were set to 0.4 and 0.7, respectively. Note that volcanic eruptions in Iceland can result in ash deposits on the snow, and lower the albedo of the resulting slush and snow cover on VGHV and lead to earlier ice-off dates (Landl et al., 2003). However, we expect this to only be important during volcanic eruptions that occurred during the winter and/or spring season and would only influence the lake water temperatures and ice-cover during that year. As our purpose is to understand how the lake responds on longer-timescales, we keep the values for albedo constant. The model was initialized using ERA-Interim daily data (1979-2018 CE; ECMWF; Dee et al., 2011) averaged over grid cells covering southwest Iceland (18.25° W-22.75° W by 63.00° N-64.50° N for a 0.75° x 0.75° grid). An initial control simulation was run for 39 years, followed by sensitivity tests where various perturbations were introduced. Results from the control simulation were compared with available meteorological data, ice-off dates from nearby lakes in Iceland, and the few observations we were able to make using satellite imagery when our study site was not obscured by clouds (Tables A2 & A3; Fig. A2). The lack of ~~an extensive dataset~~extensive observational data from VGHV prevents us from validating the

Formatted: Font color: Auto

Formatted: Font color: Auto

Formatted: Font color: Auto

~~exact~~ outputs from the lake model simulation, therefore we use the outputs from the lake model to highlight what processes ~~led~~could lead to ~~earlier~~variations in ice-off dates and ~~warmer~~ lake water temperatures during the spring season, but not to quantify the number of days or degrees that ice-off dates and temperatures, respectively, changed in the lake over the last 2,000 years.

The perturbation experiments focused on the effects of changes in seasonal air temperatures and shortwave and longwave radiation on lake surface temperatures and ice-off dates. We used instrumental data from Hella, Iceland (1958-2005 CE) to determine the magnitude of seasonal air temperature changes (Icelandic Meteorological Office). Between 1958-2004 the range of mean seasonal temperatures are as follows: winter (DJF) -3.7 °C to 1.8 °C, spring (MAM) -1.0 °C to 6.9 °C, summer (JJA) 8.8 °C to 12.0 °C, and fall (SON) -1.3 °C to 6.7 °C. To constrain the seasonality of our proxy, we perturbed the ERA interim seasonal air temperature values by -7 °C, -3 °C, 0 °C, +3 °C, and +7 °C and re-ran the lake model with the adjusted parameters. We repeated these experiments, but instead perturbed surface incident shortwave radiation to test how external forcings can drive changes in temperature. Incoming (top of the atmosphere) insolation at 63 °N has increased in winter (DJF) by 1.5 W m^{-2} and in spring (MAM) by 3.7 W m^{-2} over the past 2,000 years (Laskar et al., 2004). We therefore tested insolation forcing by perturbing seasonal changes in surface incident shortwave radiation by -4 W m^{-2}, -2 W m^{-2}, 0 W m^{-2}, +2 W m^{-2}, and +4 W m^{-2}. ~~The effects of volcanic eruptions on temperature and ice-off dates were also tested by changing shortwave radiation by -30 W m^{-2}, -10 W m^{-2}, 0 W m^{-2}, +10 W m^{-2}, and +30 W m^{-2}. These values were based on regional radiative feedback studies from the 1783 CE Laki (Oman et al., 2006) and 2010 CE Eyjafjallajökull (Hirtl et al., 2019) eruptions in Iceland.~~ It should be noted that Iceland receives minimal light during the winter months and VGHV is frozen during the winter months, so we expect little to no direct influence of insolation on lake water temperatures during winter. Shortwave radiation values for the winter (DJF) were set to 0 W m^{-2} if a negative perturbation decreased shortwave radiation below 0 W m^{-2}. To assess the effects of longwave radiation on lake water temperatures and ice-off dates, we decreased and increased incoming longwave radiation by -0.2 W m^{-2}, 0 W m^{-2}, +0.2 W m^{-2}. These values reflect the forcing from well-mixed greenhouse gas (GHG) radiation during the pre-industrial period (Schmidt et al., 2011).

3 Results

3.1 U^{K}_{37} index: corrections for species-mixing

Our U^{K}_{37} index from VGHV suggests that there was substantial variability in temperature during the last 2,000 years, but there was also variability in the community of alkenone-producers (Fig. 3a). Alkenones in VGHV surface sediments have a RIK_{37} value of 0.60 and genetic analyses confirm that Group I Isochrysidales is the main alkenone-producer (Longo et al., 2018; Richter et al., 2019). However, the RIK_{37} values increase slightly above the Group I cut-off of 0.63 about c. 500 CE, and then

Formatted: Font color: Auto
Formatted: Font color: Auto
Formatted: Font color: Red
Formatted: Font color: Red

show a more sustained increase after human settlement in Iceland (c. 870 CE), suggesting that Group II alkenone-producers were also present in the lake (Fig. 3b).

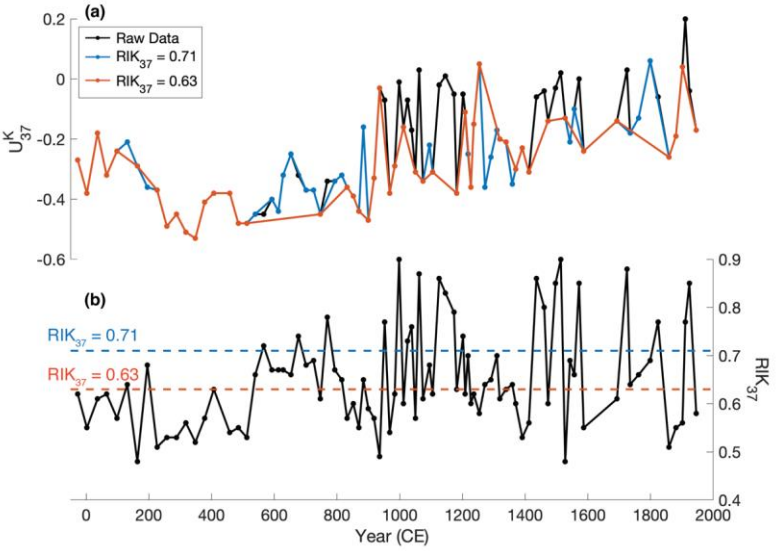

Figure 3. (a) The raw data for the U^{K}_{37} index is indicated in black, and the corrected U^{K}_{37} index with a RIK_{37} cut-off of 0.63 and 0.71 are shown in orange and blue, respectively. (b) The original RIK_{37} index is shown below for comparison with the empirical cut-off, RIK_{37} = 0.63, and cut-off for RIK_{37} = 0.71 indicated.

To evaluate the potential impacts of species mixing on the U^{K}_{37} record, samples with a high abundance of Group II alkenones were removed. We tested several different cut-offs for the RIK_{37} index and compared changes in the mean U^{K}_{37} values (Fig. 4). If no correction is applied (RIK_{37} = 1.0), then U^{K}_{37} = -0.34 ± 0.12 from 0-1000 CE and U^{K}_{37}= -0.14 ± 0.13 from 1001-2000 CE. The empirically defined cut-off of 0.63 yields a mean U^{K}_{37} index of -0.37 ± 0.12 from 0-1000 CE and -0.20 ± 0.10 from 1001-2000 CE. A less stringent RIK_{37} cut-off at 0.71, results in no significant difference in the mean or the variability of the data (0-1000 CE U^{K}_{37} = -0.36 ± 0.10 and 1001-2000 CE U^{K}_{37} = -0.21 ± 0.11). Species mixing thus affects the U^{K}_{37} temperature record, but regardless of the correction applied to the data, there is an increase in the mean U^{K}_{37} values (which we interpret as warming) from 0-1000 CE to 1001-2000 CE. To further validate our results, we also did an additional comparison using both the RIK_{37} and RIK_{28E} indices (Fig. A1). Due to lower abundance of $C_{28:3}$ Et and its isomer we had fewer datapoints for comparison, but our results still demonstrate that datapoints used in our study are predominantly produced by Group I Isochrysidales.

Formatted: Subscript
Formatted: Font color: Auto
Formatted: Subscript
Formatted: Font color: Auto
Formatted: Font color: Auto
Formatted: Subscript
Formatted: Font color: Auto

Using a RIK_{37} cut-off of 0.71, the corrected U^{K}_{37} values and RIK_{37} index are not correlated (r = 0.11, p = 0.35), indicating that species-mixing effects do not affect the final temperature calibration. The resulting U^{K}_{37} values can be interpreted as a record of temperature changes from Group I alkenones.

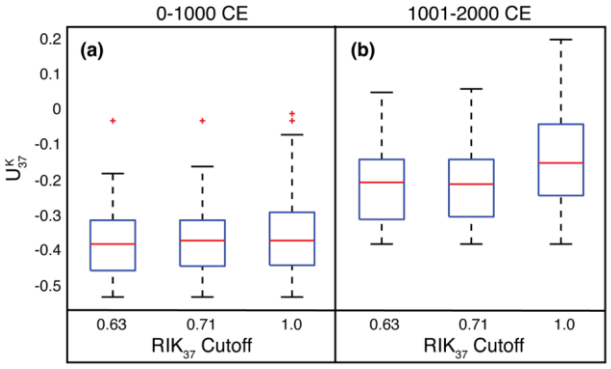

Figure 4. Different RIK_{37} cutoffs applied to the U^{K}_{37} index for (a) 0-1000 CE and (b) 1001-2000 CE. A RIK_{37} value of 1.0 indicates that the data was not corrected for species-mixing effects, while RIK_{37} = 0.63 corresponds to the empirically defined cut-off for Group I and II (Longo et al., 2018).

3.2 Controls on spring lake water temperature

Currently there are no extensive datasets on changes in lake water temperatures and/or ice-off dates for lakes (in particular lakes that are not influenced by geothermal activity or are glacial lakes that are subject to sea water intrusions) in Iceland to validate the control simulation from our lake model. However, a comparison with existing data in the literature and satellite images that were not obscured by cloud-cover suggests that the timing of the ice-out dates in our lake model (mid- to late April) and mean monthly temperatures of the surface lake water are reasonable (Tables A2 & A3; Fig. A2). We use the results from the lake model to infer what processes arecould ~~important in~~ drivinge large changes in ice-off dates and lake water temperatures, and thereby the determine the seasonal sensitivity of our proxy.

Formatted: Font color: Auto

Formatted: Font color: Auto

Formatted: Font color: Auto

Formatted: Font color: Auto

Results from the lake energy balance model show that seasonal perturbations can have a strong influence on spring lake water temperatures and ice-off dates in VGHV (Fig. 5, Tables A4~~S1 and S3~~). The control run yields an average ice-off date of April 23~~rd~~th with surface water temperatures on May 1st of~~about~~ 4.1 ± 1.5~~6.6~~ °C. Air temperature perturbations during the winter (DJF) and spring

Formatted: Font color: Auto

(MAM) alter the timing of ice-off and how rapidly surface water temperatures warm, with warmer air temperatures leading to warmer water temperatures and earlier ice-off dates (Fig. 5a-b). Changes in shortwave radiation did not have significant influence on ice-off dates or lake water temperatures; the largest response is observed in spring (MAM) ice-off dates ~~In addition, an increase in shortwave solar radiation during the spring season (MAM) leads to earlier ice-off dates and warmer lake water temperatures~~ (Fig. 5c-d, Table A5~~2~~). Shorter days during the winter months (DJF) limits the amount of shortwave radiation reaching Iceland, and therefore has a minimal influence on Icelandic temperatures (Fig. 5d ~~and f~~). ~~Shortwave radiative perturbations from volcanic eruptions during the winter season result in small changes in spring lake water temperatures and ice-off dates, while eruptions during the spring lead to much colder spring water temperatures and later ice-off dates (Fig. 5e-f, Table A2).~~ There are no competing effects of summer (JJA) or fall (SON) insolation and air temperature~~s~~ on spring lake water temperatures and the timing of ice-out. The increase in longwave radiation from GHGs during the pre-industrial period is relatively small and has no significant influence on either lake water temperatures (change from control = 0.0~~1~~ ± 2.2~~1.02~~ °C) or ice-off dates (change from control = 0.0 ~~0.03~~ ± 8.1 ~~77~~ days; Fig. A3~~1~~, Table A6~~3~~). Thus, the timing of the alkenone bloom and the water temperatures recorded by the alkenones are most likely responses to changes in air ~~temperature and temperature changes driven by shortwave radiation~~temperature during the late winter and spring season.

Formatted: Justified

Formatted: Font color: Auto

Formatted: Font color: Red

Formatted: Font color: Auto

Formatted: Font color: Auto

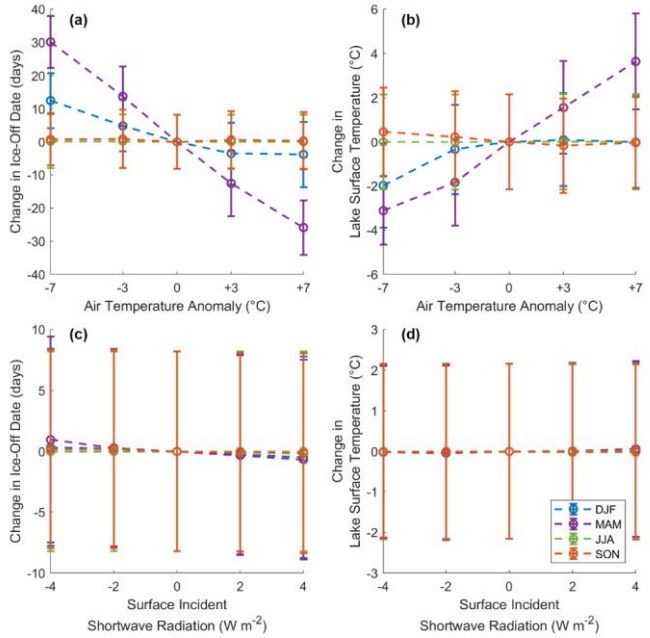

Figure 5. Lake model sensitivity tests showing the impacts of air temperature perturbations during different seasons on (a) ice-off dates and (b) lake water temperatures on May 1st. Similarly, the affects of shortwave radiation on (c) ice-off dates and (d) lake water temperatures are shown. Changes in ice-off dates and lake surface temperatures were calculated relative to the control simulation. ~~Similarly, the results for shortwave radiation perturbations that reflect changes in orbital insolation during different seasons for (c) ice-off dates and (d) lake water temperatures and changes from volcanic eruptions for (e) ice-off dates and (f) lake water temperatures are shown.~~ Seasonal changes are shown for winter (DJF, blue), spring (MAM, purple), summer (JJA, green), and fall (SON, orange).

Formatted: Font color: Auto

Formatted: Font color: Auto

Formatted: Font: 10 pt, Bold, Font color: Auto

Formatted: Normal

3.3 Long-term trends and short-term variability in the U^{K}_{37} record and temperature

The U^{K}_{37} index can provide temperature estimates using linear relationships that are calibrated in lakes with Group I alkenone-producers (D'Andrea et al. 2011, 2016; Longo et al., 2016, 2018). Existing temperature calibrations, except for the Northern Hemisphere calibration by Longo et al. (2018), for Group I are site-specific and therefore cannot be readily applied to VGHV (e.g. calibrations give estimates of 10.2 to 33.5 °C (D'Andrea et al., 2011), 7.1 to 34.4 °C (Longo et al., 2016), 4.4 to 24.5 °C (D'Andrea et al., 2016), -1.4 to 18.3 °C (calibration for Northern Hemisphere lakes by Longo et al., 2018; see Fig. A42). Most

of the variation between sites is accounted for by the y-intercept of the calibration, so the slope of Group I calibrations was suggested as a better determinant of relative temperature changes for sites lacking a site-specific calibration (D'Andrea et al., 2016). However, the slopes determined for Group I calibrations still result in a very large and likely unreasonable temperature range of 26.9 °C for U^{K}_{37} = 0.0219T (D'Andrea et al., 2016). ~~The slope determined for Group III alkenone calibrations (U^{K}_{37} = 0.0447T; D'Andrea et al., 2016) provides a more reasonable temperature range of 13.2 °C and an estimated temperature change of 8 °C from 250-350 CE to 1850-1950 CE. Given the sensitivity of VGHV lake water temperatures to winter and spring season perturbations and the large variability in winter and spring temperatures observed in the instrumental data (mean temperatures in the winter and spring (DJFMAM) season range from -2.4 °C to 3.4 °C with a seasonal variance of 13.1 °C between 1958-2004 at Hella station; Icelandic Meteorological Office), it is plausible to observe temperature swings close to 10 °C during the spring transitional season (Fig. 5b). However, the~~The amplitude of the reconstructed temperature~~s~~ is still relatively large considering that each sample is an average of 5-19 years, and most likely stems from the lack of a local calibration. These discrepancies are highlighted by the variability observed in the Northern Hemisphere calibration developed by Longo et al. (2018), where only 60% of the U^{K}_{37} index is explained by temperatures during the spring isotherm. In VGHV, the U^{K}_{37} temperature relationship could highlight the differences in the sensitivity of VGHV lake water temperatures to air temperature relative to previous studies on Group I Isochrysidales (Longo et al., 2018). Despite these differences ~~Nevertheless~~, the U^{K}_{37} index is known to be highly sensitive to temperatures in NH lakes ~~and~~and both the millennial and multidecadal ~~the~~ variability in our U^{K}_{37} index exceed~~s~~ the range of our analytical uncertainty~~;~~. We assume that, after correcting for species mixing, there are no~~t~~ environmental parameters other than temperature that affect our U^{K}_{37} record, and we ~~I, t~~therefore ~~we~~ use the U^{K}_{37} index to infer and evaluate qualitative changes in temperature trends and variability during the past 2,000 years.

The U^{K}_{37} record from VGHV, corrected for species mixing, exhibits a long-term trend towards warmer spring lake water temperatures over the last 2,000 years as well as strong multi-decadal to centennial variability (Fig. 6). The gradual warming trend in our record begins after c. 400 CE. In particular, a warmer period occurs from the start of our record to c. 200 CE, followed by a cooler period~~ing~~ from c. 250-600 CE. Temperature variability increases after c. 850 CE, and warmer periods occur between c. 850-1050 CE, c. 1100-1300 CE, and c. 1450-1550 CE. Relatively cooler periods occur at c. 1100-1200 CE, c. 1300-1450 CE, c. 1550-1750 CE, and c. 1850-1880 CE. However, caution should be used when interpreting results after c. 1400 CE because of low sampling resolution (c. 50 yrs between each sample).

4 Discussion

4.1 Regional controls on winter and spring temperatures in southwest Iceland

Results from the lake-energy balance model suggest that lake water temperatures during the spring season and the timing of ice-off in VGHV primarily respond to changes in air temperature during the winter and spring season. Air temperatures in

Formatted: Font color: Auto
Formatted: Font color: Auto
Formatted: Font color: Auto
Formatted: Font color: Auto
Formatted: Font color: Auto
Formatted: Font color: Auto
Formatted: Font color: Auto
Formatted: Line spacing: 1.5 lines

southwest Iceland are typically warmer (Vestmannaeyjar mean annual air temperature (MAAT): 4.9 ± 0.6 °C for 1878-2002) than in northern Iceland (Grímsey MAAT: 2.3 ± 1.0 °C for 1878-2002) due to the advection of the warm Irminger Current along the southern coast and lack of sea-ice formation during the winter and spring seasons (Einarsson, 1984; Hanna et al., 2004). Based on our lake model simulation, spring surface water temperatures in VGHV ~~solely~~ respond to changes during the winter and spring season because the lake re-freezes every winter and reaches minimum lake water temperatures, meaning any influence from the previous summer or fall season are negligible (e.g. Assel and Robertson, 1995). Similar lake-model parameterizations were used to simulate spring lake water temperatures in a lake in Alaska, where the lake-model was ~~v~~rigorously tested against observational data, and the authors also observed that surface water temperatures during the spring season only respond to air temperature changes during the winter and spring (DJFMAM) seasons (Longo et al., 2020). Further, an increase in winter and spring air temperatures leads to earlier ice-off dates. This is consistent with previous work in Alaska where an increase of 3 °C during the winter and spring (DJFMAM) led to an earlier simulated ice-off date by 12 days (Longo et al., 2020). Lake ice-off is expected to occur earlier during years when volcanic ash leads to "dirty" snow and lowers the albedo of the lake ice (Landl et al., 2003); however, this likely has a minimal influence on our record on 10 to 20-year timescales. This suggests that our alkenone proxy is primarily sensitive to changes in air temperatures during the winter and spring season.~~Winter-spring temperatures from VGHV warm over the past 2,000 years (Fig. 6), and our lake energy balance modelling results indicate that increasing shortwave radiation and air temperatures during the winter and spring season could result in warmer water temperatures and earlier ice-off dates. Lake water temperatures in VGHV solely respond to changes during the winter and spring season because the lake re-freezes every winter and reaches minimum lake water temperatures, meaning any influence from the previous summer or fall season are negligible (e.g. Assel and Robertson, 1995). Mean annual long-wave radiative forcing, i.e. GHGs, over the pre-industrial period has a minimal influence on water temperatures and ice-off dates. This suggests that the long-term warming trend in VGHV is driven by air temperature changes and solar insolation during the winter and spring season. However, as our record only spans the last 2,000 years, the warming trend in our record could also be a feature of the last millennium associated with regional processes.~~

The VGHV temperature record shows that winter and spring air temperatures warmed over the last millennium, whereas temperature and sea ice reconstructions suggest that summer air temperatures cooled in Northern and Western Iceland as sea ice increased and reached a maximum during the 18th and 19th centuries (Ogilvie and Jónsson, 2001; Moros et al., 2006; Massé et al., 2008; Gathorne-Hardy et al., 2009; Axford et al., 2009, 2011; Langdon et al., 2011; Cabedo-Sanz et al., 2016; Holmes et al., 2016). Paleo- and historical records, however, indicate that sea ice was only present along the southern and western coasts of Iceland, where our study site VGHV is located, during severe ice years when sea ice is advected clockwise around the country (Ogilvie, 1996; Axford et al., 2011; Cabedo-Sanz et al., 2016). Sea ice often leads to enhanced cooling in Northern Iceland relative to Southern Iceland, leading to a larger temperature gradient and differences in the rate of warming, particularly

Formatted: Font: (Default) +Headings (Times New Roman)
Formatted: Font: (Default) +Headings (Times New Roman), Font color: Auto
Formatted: Font: (Default) +Headings (Times New Roman)
Formatted: Font: (Default) +Headings (Times New Roman)
Formatted: Font: (Default) +Headings (Times New Roman), Font color: Auto
Formatted: Font: (Default) +Headings (Times New Roman)
Formatted: Font color: Auto
Formatted: Font color: Auto
Formatted: Font color: Auto
Formatted: Font color: Auto
Formatted: Font color: Auto
Formatted: Font color: Auto
Formatted: Font color: Auto
Formatted: Font color: Auto
Formatted: Font color: Auto
Formatted: Font color: Auto
Formatted: Font color: Auto
Formatted: Font color: Auto
Formatted: Font color: Auto
Formatted: Font color: Auto

during the winter and spring months (e.g. from 1871-2001 Grímsey in Northern Iceland warmed by 1.4°C and 0.6°C in winter (DJFM) and spring (MA), respectively compared to Vestmannaeyjar in Southern Iceland warmed by 2.1°C and 2.3°C in winter and spring, respectively; Hanna et al., 2004). In contrast to Northern Iceland, sea ice is therefore expected to have a smaller impact on air temperatures at our study site over the last 2,000 years.

Similar to our record from VGHV, millennial-scale changes in spring temperatures inferred from biogenic silica in western Iceland are decoupled from temperature and sea-ice changes in Northern Iceland, suggesting that spring temperatures are likely more sensitive to changes in regional SSTs (Geirsdóttir et al., 2009). SST reconstructions near southern Iceland show that surface temperatures either increased (Berner et al., 2008; Thornalley et al., 2009; Miettinen et al., 2012; Orme et al., 2018) or did not significantly change (Sicre et al., 2011; Van Nieuwenhove et al., 2018) over the last 2,000 years. Marine reconstructions of temperature from below the summer thermocline and bottom water record a decrease in mean annual temperatures over the Common Era (Thornalley et al., 2009; Ólafsdóttir et al., 2010; Moffa-Sánchez et al., 2014) as the transport of warm North Atlantic waters by the Irminger Current decreased over the last 2,000 years (Ólafsdóttir et al., 2010). The differences in proxy records could be related to differences in proxy seasonality. The different seasonal response in SSTs is observed in a gradual increase in winter and decrease in summer temperatures over the Holocene in a marine record from southern Iceland, suggesting that SSTs near southern Iceland are sensitive to both changes in changes in ocean circulation and seasonal insolation (Van Nieuwenhove et al., 2018). As the maritime climate of southern Iceland is sensitive to changes in SSTs, we would therefore expect millennial-scale changes in both ocean circulation and insolation to be reflected in the VGHV temperature record. Based on existing paleo- and historical records we conclude that sea ice feedbacks play a minor role in driving long-term changes in winter and spring temperatures at our study site, whereas an increase in SSTs along the southern coast could contribute to the warming trend observed in our record. ~~Iceland has a maritime climate and also sits near the edge of the Arctic sea ice; therefore, air temperatures are sensitive to regional sea-ice feedbacks and variations in sea surface temperatures (SSTs). The VGHV temperature record shows that winter and spring air temperatures warmed over the last millennium, whereas temperature and sea ice reconstructions suggest that summer air temperatures cooled in Northern and Western Iceland as sea ice increased with the coldest period occurring during the 18th and 19th centuries (Ogilvie and Jónsson, 2001; Moros et al., 2006; Massé et al., 2008; Gathorne-Hardy et al., 2009; Axford et al., 2009, 2011; Langdon et al., 2011; Cabedo-Sanz et al., 2016; Holmes et al., 2016). Paleo- and historical records, however, indicate that sea ice was only present along the southern and western coasts of Iceland, where our study site VGHV is located, during severe ice years when sea ice is advected clockwise around the country (Ogilvie, 1996; Axford et al., 2011; Cabedo-Sanz et al., 2016). Similarly, millennial-scale changes in spring temperatures inferred from biogenic silica in western Iceland are decoupled from temperature and sea-ice changes in Northern Iceland, suggesting that spring temperatures are likely more sensitive to changes in regional SSTs (Geirsdóttir et al., 2009). SST reconstructions near southern Iceland show that surface temperatures either increased (Berner et al., 2008; Thornalley et al., 2009; Miettinen et al., 2012; Orme et al., 2018) or did not significantly change (Sicre et al., 2011; Van Nieuwenhove et al., 2018) over the last 2,000 years. Marine reconstructions of temperature from below the summer~~

Formatted: Font color: Auto

Formatted: Font: (Default) +Headings (Times New Roman), Font color: Auto

Formatted: Font color: Auto

Formatted: Font: (Default) +Headings (Times New Roman), Font color: Auto

Formatted: Font color: Auto

Formatted: Font: (Default) +Headings (Times New Roman), Font color: Auto

Formatted: Font color: Auto

Formatted: Font color: Auto

~~thermocline and bottom water record a decrease in mean annual temperatures over the Common Era (Thornalley et al., 2009; Ólafsdóttir et al., 2010; Moffa-Sánchez et al., 2014) as the transport of warm North Atlantic Current waters by the Irminger Current decreased over the last 2,000 years (Ólafsdóttir et al., 2010). Based on existing paleo- and historical records we conclude that sea ice feedbacks only play a minor role in driving long-term changes in winter and spring temperatures at our study site, whereas an increase in SSTs along the southern coast could contribute to the warming trend observed in our record. However, discrepancies in existing proxy records makes it difficult to correlate changes in SSTs to changes in winter and spring temperatures at VGHV.~~

Formatted: Font color: Auto

Formatted: Font: Not Bold

Formatted: Line spacing: 1.5 lines

4.~~2~~1 Long-term seasonal climate trends in North ~~Atlantic~~ Hemisphere paleoclimate records

Mean annual temperature syntheses from the NH exhibit a long-term cooling trend over the last 2,000 years (Kaufman et al., 2009; PAGES 2K Consortium, 2013, 2019) that is often interpreted as a response to decreasing summer insolation (Kaufman et al., 2009) and/or increased volcanic activity during the LIA (Miller et al., 2012). ~~Climate model simulations suggest that solar variability acts as a secondary source of variability and land use changes may be important for explaining some of the changes in NH surface temperatures between the MCA and LIA, whereas increases in greenhouse gases remain stable until the late 19th century (Otto-Bliesner et al., 2016).~~ The magnitude of the cooling trend ~~and centennial and multi-decadal changes~~ differs among global temperature reconstructions (PAGES 2K Consortium, 2019) and is often larger in NH temperature reconstructions compared to climate model simulations (Rehfeld et al., 2016; Ljungqvist et al., 2019). The discrepancies in temperature reconstructions and climate models could stem from a warm season bias in NH proxy reconstructions, leading to an overestimation of changes in mean annual and cold season temperatures in proxy reconstructions compared to climate model simulations (Liu et al., 2014; Rehfeld et al., 2016; PAGES 2K Consortium, 2019).

The distinct warming trend in the winter-spring temperature reconstruction from VGHV could provide new insights into the mechanisms that influence cold season temperatures in the North Atlantic region. As discussed in the previous section, the maritime climate of southern Iceland, and therefore the temperature recorded at our study site, reflect variability in seasonal SSTs that are driven by changes in ocean circulation and seasonal insolation. In contrast, mean annual long-wave radiative forcing, i.e. GHGs, over the pre-industrial period has a minimal influence on water temperatures and ice-off dates in VGHV.

Formatted: Font color: Auto

Formatted: Font color: Red

~~Winter-spring temperatures from VGHV warm over the past 2,000 years (Fig. 6), and our lake energy balance modelling results indicate that increasing shortwave radiation and air temperatures during the winter and spring season could result in warmer water temperatures and earlier ice-off dates. Lake water temperatures in VGHV solely respond to changes during the winter and spring season because the lake re-freezes every winter and reaches minimum lake water temperatures, meaning any influence from the previous summer or fall season are negligible (e.g. Assel and Robertson, 1995). Mean annual long-wave~~

radiative forcing, i.e. GHGs, over the pre-industrial period has a minimal influence on water temperatures and ice-off dates. This suggests that the long-term warming trend in VGHV is driven by air temperature changes and solar insolation during the winter and spring season. However, as our record only spans the last 2,000 years, the warming trend in our record could also be a feature of the last millennium associated with regional processes.

Iceland has a maritime climate and also sits near the edge of the Arctic sea ice; therefore, air temperatures are sensitive to regional sea-ice feedbacks and variations in sea surface temperatures (SSTs). The VGHV temperature record shows that winter and spring air temperatures warmed over the last millennium, whereas temperature and sea ice reconstructions suggest that summer air temperatures cooled in Northern and Western Iceland as sea ice increased with the coldest period occurring during the 18th and 19th centuries (Ogilvie and Jónsson, 2001; Moros et al., 2006; Massé et al., 2008; Cathorne-Hardy et al., 2009; Axford et al., 2009, 2011; Langdon et al., 2011; Cabedo-Sanz et al., 2016; Holmes et al., 2016). Paleo- and historical records, however, indicate that sea ice was only present along the southern and western coasts of Iceland, where our study site VGHV is located, during severe ice years when sea ice is advected clockwise around the country (Ogilvie, 1996; Axford et al., 2011; Cabedo-Sanz et al., 2016). Similarly, millennial-scale changes in spring temperatures inferred from biogenic silica in western Iceland are decoupled from temperature and sea-ice changes in Northern Iceland, suggesting that spring temperatures are likely more sensitive to changes in regional SSTs (Geirsdóttir et al., 2009). SST reconstructions near southern Iceland show that surface temperatures either increased (Berner et al., 2008; Thornalley et al., 2009; Miettinen et al., 2012; Orme et al., 2018) or did not significantly change (Sicre et al., 2011; Van Nieuwenhove et al., 2018) over the last 2,000 years. Marine reconstructions of temperature from below the summer thermocline and bottom water record a decrease in mean annual temperatures over the Common Era (Thornalley et al., 2009; Ólafsdóttir et al., 2010; Moffa-Sánchez et al., 2014) as the transport of warm North Atlantic Current waters by the Irminger Current decreased over the last 2,000 years (Ólafsdóttir et al., 2010). Based on existing paleo- and historical records we conclude that sea ice feedbacks only play a minor role in driving long-term changes in winter and spring temperatures at our study site, whereas an increase in SSTs along the southern coast could contribute to the warming trend observed in our record. However, discrepancies in existing proxy records makes it difficult to correlate changes in SSTs to changes in winter and spring temperatures at VGHV.

Long-term warming trends over the Holocene and the Common Era were also observed in other records of cold-season temperatures in the NH. For instance, pollen records of cold-season temperatures from North America and Europe (Mauri et al., 2015; Marsicek et al., 2018) and an alkenone reconstruction of winter-spring temperatures from Alaska (Longo et al., 2020) suggest that increasing winter and spring orbital insolation over the Holocene drove warming during the winter and spring season. Winter warming over the Holocene, including the Common Era, was also inferred from chrysophyte cysts in Spain (Pla and Catalan, 2005), ice-wedge records in the Siberian Arctic (Meyer et al., 2015; Opel et al., 2017), and a speleothem record from the Ural Mountains in Russia (Baker et al., 2017). A marine record directly south of Iceland from the North Atlantic subpolar gyre, records winter SSTs that are on average warmer over the last 2,000 years relative to the early to mid-

Holocene (Van Nieuwenhove et al., 2018). In each of these studies, insolation and/or rising greenhouse gases are proposed as the primary mechanisms driving changes in seasonal temperatures~~, supporting the results of our energy balance model~~.

Although there are existing reconstructions of NH winter and spring temperatures during the Common Era, the high-resolution reconstruction of winter-spring temperatures from VGHV is one of the few sites in the n~~N~~orthern high latitudes where the effects of seasonal insolation ~~-~~on winter and spring temperatures can be tested without having to account for the influence of confounding factors, such as precipitation, on proxy records. For instance, varve thickness records have been interpreted to reflect winter temperatures but might be influenced by human activities in the catchment area, variations in snow accumulation, the timing of spring melt, and changes in precipitation (Ojala and Alenius, 2005; Haltia-Hovi et al., 2007). Varve thickness records from the Arctic that record changes in snow or glacial melt are also used to infer long-term cooling during the melt season; however, the melt season in the high Arctic often extends well into the summer months (Cook et al., 2009; Larsen et al., 2011) and can be affected by Arctic summer hydrology. Water isotope records from ice cores from Svalbard and a stalagmite from the Central Alps are sensitive to winter air temperatures during the instrumental period, but changes in the moisture source and seasonality of precipitation over time can alter long-term temperature interpretations (Isaksson et al., 2005; Mangini et al., 2005; Divine et al., 2011a, b). Although our record lacks a local calibration, we argue that the U^{K}_{37} record from VGHV provides a robust, albeit qualitative, record of winter-spring temperatures given the unique seasonal growth ecology of Group I haptophytes in NH lakes. The warming trend observed in our record from Iceland and other records of cold-season temperatures from the NH suggest that long-term temperature changes are driven by a common forcing, orbitally-driven changes in winter and spring insolation, during the Holocene (Mauri et al., 2015; Meyer et al., 2015; Baker et al., 2017; Marsicek et al., 2018; Van Nieuwenhove et al., 2018; Longo et al., 2020) and during the Common Era (Pla and Catalan, 2005; Meyer et al., 2015; Baker et al., 2017; Opel et al., 2017).

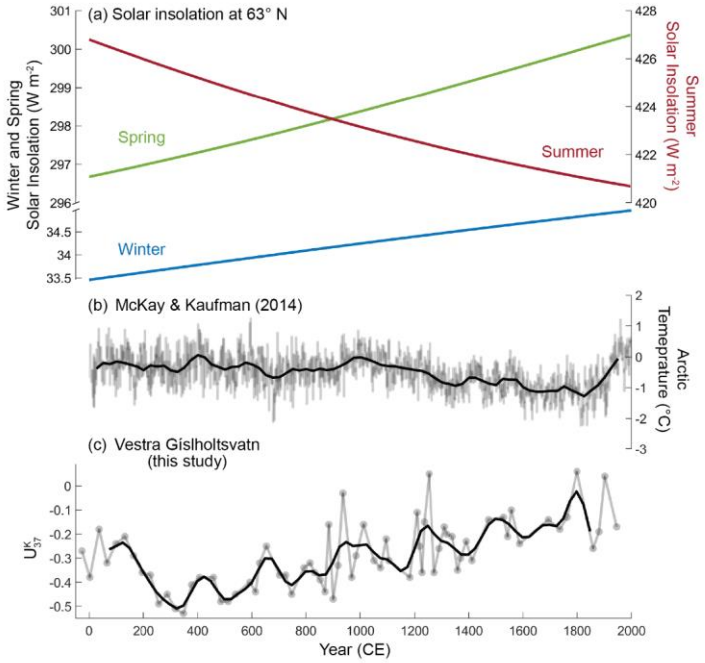

485 **Figure 6.** ~~**(a) Changes in solar insolation at 63ºN for winter (DJF), spring (MAM), and summer (JJA) are shown for the past 2,000 years (Laskar et al., 2004). In addition, (b) a compilation of Arctic temperature reconstructions (McKay and Kaufman, 2014) is shown for comparison with the (c) winter-spring temperature reconstruction from VGHV (the thick black lines for panels (b) and (c) are lowpass filters with data resampled to every 25 years to capture the low-frequency variability of the datasets).**~~ **(a) Changes in solar insolation at 63ºN for winter (DJF), spring (MAM), and summer (JJA) are shown for the past 2,000 years (Laskar et al.,**
490 **2004). In addition, (b) a compilation of Arctic temperature reconstructions (McKay and Kaufman, 2014) is shown for comparison with the (c) winter-spring temperature reconstruction from VGHV. The thick black lines correspond to lowpass filters (every 25 years) applied to the Arctic dataset and VGHV record.**

~~The warming trend observed in our new record from Iceland and other records of cold-season temperatures from the NH~~
495 ~~suggest that long-term temperature changes are driven by a common forcing, orbitally-driven changes in winter and spring insolation, during the Holocene (Mauri et al., 2015; Meyer et al., 2015; Baker et al., 2017; Marsicek et al., 2018; Van Nieuwenhove et al., 2018; Longo et al., 2020) and during the Common Era (Pla and Catalan, 2005; Meyer et al., 2015; Baker~

et al., 2017; Opel et al., 2017). Our lake model results confirm that water temperatures are sensitive to seasonal air temperatures and indirectly respond to perturbations in shortwave radiation, indicating that the long-term warming trend observed in the VGHV record can in part be attributed to increasing late-winter and early spring insolation.

4.32 Seasonal mMulti-decadal to centennial climate variability in winter-spring temperature in the North Atlantic

Formatted: Font color: Auto

The VGHV reconstruction of winter-spring temperatures provides an opportunity to test how changes in internal climate variability and external forcings (volcanic eruptions and total solar irradiance, or TSI) influence temperature changes during the winter and spring seasons in the North Atlantic region. This is important for understanding on multi-decadal to centennial climate changes during the winter and spring seasonstimescales and the role of the Atlantic Multi-decadal Variability/Oscillation (AMV/AMO), a low-frequency basin-wide North Atlantic SST anomaly that varies in response to external forcings and internal variability, in driving and/or responding to changes during the winter (Kerr, 2000; Wang et al., 2017; Yeager and Robson, 2017). The NAO, defined by differences in sea-level pressure between the subpolar low and the subtropical high, is a major source of atmospheric variability during the winter months (Hurrell, 1995). Although the NAO is mainly associated with interannual timescales, there is also evidence that NAO-like patterns can emerge at multi-annual to centennial timescales, potentially linked to coupled changes in oceanic and atmospheric circulation (Visbeck et al., 2003; Delworth et al., 2016; Yeager and Robson, 2017). For instance, a positive (negative) NAO phase that persists for multiple winters can lead to increased (decreased) deepwater formation in the Labrador Sea and strengthening (weakening) of the subpolar gyre (SPG) and the meridional overturning circulation, thereby resulting in an increased (decreased) transport of warm waters towards the poles (Eden and Jung, 2001; Visbeck et al., 2003; Latif et al., 2006; Moffa-Sánchez and Hall, 2017). Alternatively, an increase in the southward transport of polar waters could also result in a reduction of deepwater formation in the Labrador Sea and a weaker subpolar gyreSPG, leading to a decrease in northward oceanic heat transport and centennial cooling of ocean and regional air temperatures but warming of SSTs south of Iceland (Moffa-Sánchez and Hall, 2017; Moreno-Chamarro et al., 2017).

Whether forced or unforced, variability in winter atmospheric circulation, including the NAO, and sea ice extent are often linked to multi-decadal and centennial climate change in the North Atlantic region, particularly over Iceland (e.g. Hanna et al., 2006; Massé et al., 2008; Wang et al., 2017; Yeager and Robson, 2017). In the VGHV record of winter-spring temperatures there is a sharp decrease in the $U^{K}_{37'}$ index c. 250 CE and a corresponding increase in drift ice along the North Icelandic shelf (c. 400-900 CE (), which coincides with the Roman Warm Period to Dark Ages Cold Period (DACP) transition (Fig. 7; Moros et al., 2006; Cabedo-Sanz et al., 2016). Cooling during the DACP isthis time period is typically attributed to volcanic eruptions and a minimum in solar activity (c. 400-700 CE; Fig. 7a-b); however, the DACP wasthis cold interval was not uniform across the NH and records differ as to when peak cooling occurred (Helama et al., 2017). For instance, a colder interval is observed in a marine SST record from the south of Iceland c. 200-400 CE, whereas there is no distinct or prolonged cooling in in Iceland SST records during the DACPfrom the North Icelandic shelf (Fig. 7c and d; Sicre et al., 2008, 2011; Miettinen et al., 2012;

Jiang et al., 2015) or in summer temperature records from Icelandic lakes (Gathorne-Hardy et al., 2009; Axford et al., 2009). In contrast, terrestrial records from the Arctic and Northern Europe indicate that temperatures were on average cooler between c. 450-700 CE and c. 500-650 CE, respectively (Kaufman et al., 2009; Sigl et al., 2015; Helama et al., 2017). The heterogenous temperature response in the North Atlantic region could be associated with a strengthening of the SPG between c. 200-400 CE ~~A peak in sea ice is also recorded in a high-resolution IP_{25} reconstruction from the North Icelandic shelf (Cabedo-Sanz et al., 2016), whereas lower resolution records that were developed using quartz and IP_{25} show a gradual increase in sea ice after c. 400 CE but not distinct peak (Moros et al., 2006; Cabedo-Sanz et al., 2016).~~ , resulting in increased oceanic meridional heat transport to Northern Europe and colder SSTs near southern Iceland (Miettinen et al., 2012; Moffa-Sánchez and Hall, 2017). After c. 400 CE there is evidence of increased salinity and warming SSTs south of Iceland, that are associated with a gradual weakening of the SPG and contributed to a return to warmer temperatures in our VGHV record (Thornalley et al., 2009; Moffa-Sánchez and Hall, 2017; Moreno-Chamarro et al., 2017). A weaker SPG after c. 400 CE would also result in cooler Nordic waters and contribute to the cooler climate conditions observed in Northern Europe c. 500-650 CE (Miettinen et al., 2012; Helama et al., 2017; Moffa-Sánchez and Hall, 2017). ~~Increases in sea ice during this time period are attributed to a southward shift of the subpolar front and the increased advection of drift ice from Greenland to Northern Iceland (Moros et al., 2006; Cabedo-Sanz et al., 2016), leading to cooler winter and spring temperatures in Northern and Southern Iceland.~~

Winter and spring temperatures in VGHV were on average higher between c. 880-1100 CE than temperatures during the DACP but were not stable or particularly warm, unlike the climate usually associated with the Norse settlement of Iceland between c. 870-1100 CE (Fig. 7; Ogilvie et al., 2000). This time period corresponds to a peak in TSI and weak volcanic activity (PAGES 2K Consortium, 2013), ~~which could have triggered a positive phase in the AMV/AMO (Otto-Bliesner et al., 2016; Wang et al., 2017)~~ and warmer summer and annual SSTs near Northern and Southern Iceland (Sicre et al., 2008, 2011; Justwan et al., 2008; Ran et al., 2011). Summer temperature reconstructions from lakes in Northern and Western Iceland also record warmer temperatures c. 800-1300 CE but with distinct cold excursions occurring between c. 1000-1300 CE (Axford et al., 2009; Gathorne-Hardy et al., 2009; Holmes et al., 2016). Peaks in sea ice, however, are only noted after c. 1200 CE (Ogilvie, 1992; Ogilvie and Jónsson, 2001; Massé et al., 2008; Cabedo-Sanz et al., 2016), suggesting that an alternative mechanism, such as the NAO, may be responsible for the short-term variability observed in terrestrial temperature records from Iceland during this time period.

The 14^{th}-15^{th} centuries mark the start of the LIA and are often associated with a colder-than-average climate in Iceland (Ogilvie, 1984; Ogilvie and Jónsson, 2001). In contrast, the VGHV record indicates there was no prolonged cold period during the winter and spring season at our study site between c. 1300-1800 CE, which could indicate a continued response to the warming observed in SSTs south of Iceland (Thornalley et al., 2009; Miettinen et al., 2012).~~: Rather, temperatures inferred from the VGHV record varied on multi-decadal to centennial timescales.~~ Cooling during this time period is associated with major

Formatted: Font color: Auto
Formatted: Font color: Auto
Formatted: Font color: Auto
Formatted: Font color: Auto
Formatted: Font color: Auto

volcanic eruptions and decreases in TSI (PAGES 2K Consortium, 2013; Otto-Bliesner et al., 2016) that ~~most likely resulted in a negative AMV/AMO phase (Wang et al., 2017) and~~led to an ~~temporary~~ increase~~s~~ in sea ice (Fig. 7; Moros et al., 2006; Massé et al., 2008; Cabedo-Sanz et al., 2016~~)~~ and~~). In marine records from the North Icelandic shelf, this led to~~ cooling of summer/annual SSTs between c. 1400-1900 CE along the North Icelandic shelf (Fig. 7c and e; Jiang et al., 2005, 2015; Sicre et al., 2008; Ran et al., 2011). A record of subsurface winter temperatures inferred from glycerol dialkyl glycerol tetraethers (GDGTs) along the North Icelandic shelf also record cold excursions between 1200-1900 CE, with increased sea ice cover that resulted in insulation-induced warming between c. 1550-1750 CE (Harning et al., 2019). The inconsistent response in VGHV temperatures to volcanic eruptions and solar minima between c. 1300-1800 CE could be associated with stochastic climate processes, such as the NAO, or a continued weakening of the SPG that counteracted the effects of negative radiative forcings and led to winter and spring warming over southern Iceland rather than cooling as observed in Northern Iceland.

On multi-decadal to centennial timescales, changes in the VGHV record do not consistently correspond to major temperature anomalies observed during the summer months. The differences in seasonal climate responses to external forcings imply that the regional manifestation of these events depends on the initial state of the atmosphere and ocean but are also modulated by internal climate variability and changes in SSTs near southern Iceland associated with the SPG.

Formatted: Font color: Auto

Formatted: Font color: Auto

Formatted: Font color: Auto

Formatted: Font color: Auto

Formatted: Font color: Red

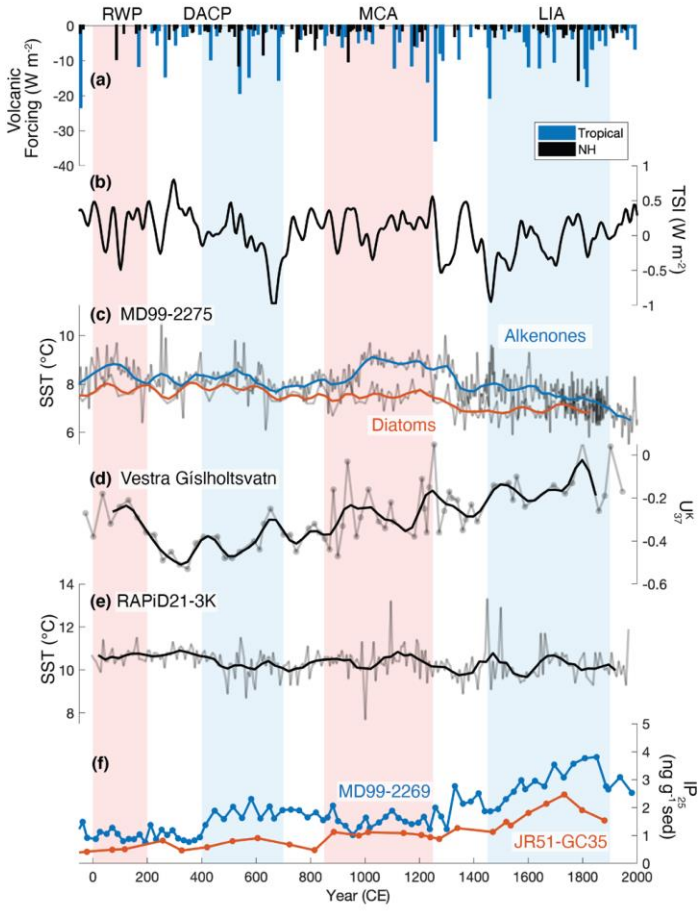

Figure 7. Major changes in radiative forcings over the past 2,000 years, including (a) volcanic forcing from tropical and NH eruptions (Sigl et al., 2015) and (b) changes in total solar irradiance (TSI; Steinhilber et al., 2009) are shown. Marine and terrestrial reconstructions from Iceland are shown, including (c) alkenone and diatom sea surface temperature (SST) reconstructions from core MD99-2275 on the North Icelandic shelf (Sicre et al., 2008; Jiang et al., 2015), (d) an alkenone winter-spring temperature reconstruction from VGHV in southwest Iceland (this study), (e) an alkenone SST record from core RAPiD21-3K in the sub-polar North Atlantic (Sicre et al., 2011), and (f) sea-ice reconstructions developed using IP_{25} from cores MD99-2269 (blue) and JR51-GC35 (orange) from the North Icelandic shelf (Cabedo-Sanz et al., 2016). The timing of major climate anomalies inferred from Icelandic climate records include: the Roman Warm Period (RWP, c. 0-200 CE), Dark Ages Cold Period (c. 400-700 CE), Medieval Climate Anomaly (MCA, c. 850-1250 CE), and Little Ice Age (LIA, c. 1450-1900 CE).

~~In the VGHV record, multi-decadal variability and an inconsistent temperature response to major radiative forcings during the LIA suggest that temperature anomalies during the winter and spring are driven by both forced and unforced variability. For instance, the strong negative radiative forcing after the Samalas eruption (1258 CE) and the Wolf solar minimum (c. 1280-1350 CE) correspond to an increase in drift ice along the North Icelandic shelf (Fig. 7; Massé et al., 2008; Cabedo-Sanz et al., 2016), a cold excursion in winter subsurface temperatures from the North Icelandic shelf c. 1350-1500 CE (Harning et al 2019), and cooling in the VGHV temperature record. Similarly, the cumulative effects of the Dalton solar minimum c. 1790-1830 CE and multiple major volcanic eruptions (i.e., Laki 1783 CE, unidentified 1809 CE, and Tambora 1815 CE; Sigl et al., 2015; Toohey and Sigl, 2017) in the late 18th and early 19th century could have resulted in enhanced sea ice feedbacks and cooling in VGHV temperatures between c. 1800-1900 CE (Massé et al., 2008; Zanchettin et al., 2012; Cabedo-Sanz et al., 2016). The inconsistent response in VGHV temperatures to volcanic eruptions and solar minima between c. 1450-1750 CE could be associated with stochastic climate processes, such as the NAO, that counteracted the effects of negative radiative forcings and led to winter warming over Iceland rather than cooling.~~

~~On multi-decadal to centennial timescales, changes in the VGHV record do not consistently correspond to major temperature anomalies observed during the summer months. The differences in seasonal climate responses to external forcings imply that the regional manifestation of these events depends on the initial state of the atmosphere and ocean but is also modulated by internal climate variability (Zanchettin et al., 2012; Otto-Bliesner et al., 2016; Anchukaitis et al., 2019).~~

5 Conclusions

The most striking feature of the VGHV record of winter-spring temperatures is a long-term warming trend from c. 250 CE to the present. Gradual warming in winter and spring ~~cold-season~~ temperatures is most likely associated with gradual warming of SSTs near Southern Iceland that are responding to ~~driven by~~ increasing winter and spring solar insolation over the last 2,000 years. This~~, and~~ contrasts with inferences of mean annual and summer time warming elsewhere in the NH. On multi-decadal to centennial timescales winter-spring temperatures are ~~sensitive to strong radiative perturbations, but~~ regional temperature responses to strong radiative forcings ~~can be~~ are often masked by internal climate variability or changes in ocean circulation. These processes can cause regional differences in temperature and strong contrasts between winter and spring, summer, and mean annual temperatures. In general, this highlights a need for more winter and spring temperature reconstructions to improve our understanding of the magnitude and direction of cold-season temperature changes over the Common Era.

Formatted: Line spacing: single
Formatted: Font color: Red
Formatted: Font color: Auto
Formatted: Font color: Auto
Formatted: Font color: Auto
Formatted: Font color: Auto
Formatted: Font color: Auto
Formatted: Font color: Auto
Formatted: Font color: Auto
Formatted: Font color: Auto
Formatted: Font color: Auto

Appendix A

Table A1. Lake specific parameters for the model set up and references used to constrain the parameters.

Parameter	Value	Source
Obliquity	23.4°	-
Latitude	63.9°N	Blair et al. (2015)
Longitude	23.9°W	Blair et al. (2015)
Local time (GMT)	+0	-
Max. depth (m)	15	Blair et al. (2015)
Elevation of basin bottom (m.a.s.l)	61	Blair et al. (2015)
Catchment + Lake area (hectares)	157	Blair et al. (2015)
Neutral drag coefficient	0.002	Longo et al. (2020)
Shortwave extinction coefficient (1/m)	0.3	Determined using $I_z/I_0 = e^{-\eta z}$ where $I_z/I_0 = 0.01$, z = 15 m, and η is the extinction coefficient (Descy et al., 2006;
Fraction of advected air over lake	0.3	Dee et al., 2018; Longo et al. 2020)
Albedo of melting snow (slush)	0.4*	Longo et al. (2020)
Albedo of non-melting snow	0.7*	Longo et al. (2020)
Average depth (m)	14	Blair et al. (2015)
Salinity (ppt)	0.0	Longo et al. (2018)

**Note: the albedo will be lower if there was a volcanic eruption that led to "dirty" snow and/or slush (Landl et al., 2003).*

Formatted: Font: Bold, Not Italic

Formatted: Font: Bold, Not Italic

Formatted: Font: Bold, Not Italic

Formatted: Font: Not Italic

Formatted: Font: Not Bold

Table A2. Outputs for lake model simulation and comparison with available observational data from Iceland.

Lake	Physical properties					Lake Surface Temp. (°C)		Ice cover		Citations
	Lat. (°N)	Lon. (°W)	Alt (m.a.sl.)	Max. Depth (m)	Area (km^2)	Summer (JJA)	Winter (DJF)	Duration	Ice-out	
Simulation for VGHV	63.9	23.9	61	14	1.57	9-10	0	Dec.-Apr.	mid to late Apr. (avg. Apr. 23rd)	Blair et al. (2015), this study
Elliðavatn	64.1	21.8	75	2.3	2.02	12-16	0-2	N/A	N/A	Malmquist et al. (2009)
Mývatn	65.6	17.0	278	4.2	53	8-13	0-3	Oct.-May	May	Ólafsson (1979); Andradóttir (2012)
Thingvallavatn	64.2	21.1	100.5	114	82	10-11	1-2	Jan.-Apr.	Apr. (avg. Apr. 12th)	Adalsteinsson et al. (1992); Andradóttir (2012)
Skorarvatn	66.3	22.3	183	N/A	1.92	8*	-2*	N/A	Apr.-May	Harning et al. (2020)

*Note: Skorarvatn temperatures are air temperatures that were based on a nearby meteorological station (Æðey) and were adjusted using the lapse rate for Skorarvatn.

Formatted: Font: Bold, Not Italic
Formatted: Font: Not Italic
Formatted: Font: Bold, Not Italic
Formatted: Font: Bold, Not Italic
Formatted: Font: Bold, Not Italic
Formatted: Font: Bold, Not Italic
Formatted: Font: Not Italic
Formatted: Font: Not Bold, Not Italic
Formatted: Font: Not Bold, Not Italic
Formatted: Font: Not Bold, Not Italic
Formatted: Font: Not Bold, Not Italic
Formatted: Font: Not Bold, Not Italic
Formatted: Font: Not Italic
Formatted: Font: Not Bold, Not Italic
Formatted: Font: Not Italic
Formatted: Font: Not Bold, Not Italic
Formatted: Font: Not Bold, Not Italic
Formatted: Font: Not Italic
Formatted: Font: Not Bold, Not Italic
Formatted: Font: Not Bold, Not Italic
Formatted: Font: Not Bold, Not Italic
Formatted: Font: 8 pt, Not Bold
Formatted: Font: Not Bold, Not Italic
Formatted: Font: Not Bold, Not Italic
Formatted: Font: Not Italic
Formatted: Font: Not Bold, Not Italic
Formatted: Font: Not Bold, Not Italic

Table A3. Ice-out dates determined using satellite imagery (Planet Labs Inc.). Due to cloud-cover we could not determine the exact dates of ice-off. We recorded the last day we observed ice on VGHV and the first day where we were able to observe VGHV as being completely ice-free.

Year	Last day ice observed on lake	First day no ice observed on lake
2012	N/A	April 22
2014	March 28	April 13
2016	March 17	April 7
2018	March 31	April 23
2019	March 30	April 5
VGHV Simulated		**Average: April 23**

Table A4. Results from the lake energy-balance model for air temperature perturbations showing the change in ice-off dates and lake water temperatures relative to the control simulation (average ice-off date: Apr. 23 ± 6 days, average lake water temperature = 4.1 ± 1.5 °C).

Temperature Perturbation	Change in Ice-off Date (days)	Change in Surface Water Temperatures on May 1st (°C)
DJF -7 °C	12.5 ± 8.3	-2.0 ± 1.9
DJF -3 °C	4.9 ± 7.8	-0.3 ± 2.0
DJF +3 °C	-3.5 ± 9.3	0.1 ± 2.1
DJF +7 °C	-3.8 ± 9.9	0.0 ± 2.1
MAM -7 °C	30.1 ± 7.8	-3.1 ± 1.5
MAM -3 °C	13.8 ± 9.0	-1.8 ± 2.0
MAM +3 °C	-12.6 ± 9.9	1.6 ± 2.1
MAM +7 °C	-25.9 ± 8.2	3.6 ± 2.2
JJA -7 °C	0.2 ± 8.1	0.0 ± 2.2
JJA -3 °C	0.2 ± 8.1	0.0 ± 2.2
JJA +3 °C	0.0 ± 8.2	0.0 ± 2.2
JJA +7 °C	0.0 ± 8.2	0.0 ± 2.2
SON -7 °C	0.8 ± 8.0	0.5 ± 2.0
SON -3 °C	0.9 ± 8.8	0.2 ± 2.1
SON +3 °C	0.6 ± 8.7	-0.2 ± 2.1
SON +7 °C	0.4 ± 8.7	0.0 ± 2.1

Table A5. Results from the lake energy-balance model for shortwave radiation perturbations showing the change in ice-off dates and lake water temperatures relative to the control simulation (average ice-off date: Apr. 23 ± 6 days, average lake water temperature = 4.1 ± 1.5 °C).

Shortwave Solar Radiation Perturbation	Change in Ice-off Date (days)	Change in Surface Water Temperatures on May 1st (°C)
DJF - 4 W m^{-2}	0.3 ± 8.1	0.0 ± 2.2
DJF - 2W m^{-2}	0.2 ± 8.1	0.0 ± 2.2
DJF + 2 W m^{-2}	-0.2 ± 8.2	0.0 ± 2.2
DJF + 4 W m^{-2}	-0.5 ± 8.3	0.0 ± 2.2
MAM - 4 W m^{-2}	1.0 ± 8.4	0.0 ± 2.1
MAM - 2 W m^{-2}	0.3 ± 8.1	0.0 ± 2.2
MAM + 2 W m^{-2}	-0.3 ± 8.2	0.0 ± 2.2
MAM + 4 W m^{-2}	-0.7 ± 8.2	0.1 ± 2.2
JJA - 4 W m^{-2}	0.0 ± 8.2	0.0 ± 2.2
JJA - 2 W m^{-2}	0.0 ± 8.2	0.0 ± 2.2
JJA + 2 W m^{-2}	0.0 ± 8.2	0.0 ± 2.2
JJA + 4 W m^{-2}	0.0 ± 8.2	0.0 ± 2.2
SON - 4 W m^{-2}	0.2 ± 8.1	0.0 ± 2.2
SON - 2 W m^{-2}	0.2 ± 8.1	0.0 ± 2.2
SON + 2 W m^{-2}	-0.1 ± 8.2	0.0 ± 2.2
SON + 4 W m^{-2}	-0.2 ± 8.2	0.0 ± 2.2

Table A6. Results from the lake energy-balance model for longwave radiation perturbations showing the change in ice-off dates and lake water temperatures relative to the control simulation (average ice-off date: Apr. 23 ± 6 days, average lake water temperature = 4.1 ± 1.5 °C).

Longwave Radiation Perturbation	Change in Ice-off Date (days)	Change in Surface Water Temperatures on May 1st (°C)
-0.2 W m^{-2}	0.2 ± 8.1	0.0 ± 2.2
+0.2 W m^{-2}	0.0 ± 8.2	0.0 ± 2.2

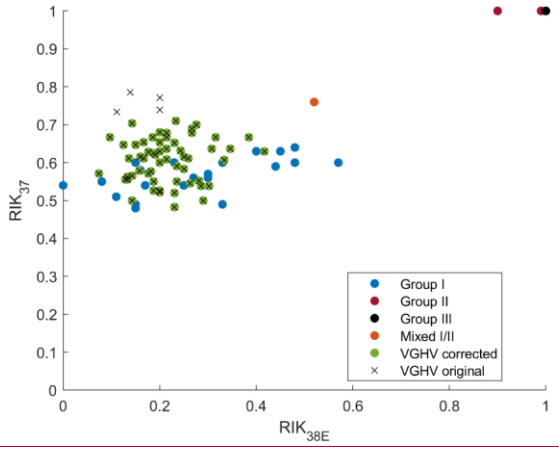

Figure A1. Comparison of RIK_{37} and RIK_{38E} values for different alkenone distributions. Group I alkenone values (blue) and a mixed sample containing Group I and II (orange) are from the Northern Hemisphere and Northern Alaska datasets (Longo et al., 2016, 2018). The Group II and III values were determined from cultures (see Longo et al. 2018). The original VGHV alkenone distributions are indicated by an X (these points only include samples where we were able to reliably identify and quantify $C_{38:3}$Et and its isomer). The VGHV alkenones that were corrected for Group II are shown in green.

Formatted: Font: Bold, Not Italic

Formatted: Font: Not Italic

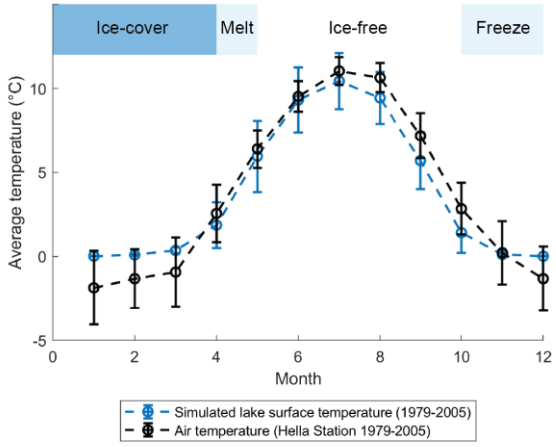

Figure A2, Comparison of simulated lake surface water temperatures for VGHV (blue) and air temperatures from a nearby meteorological station (Hella Station) for the period of 1979-2005. The average duration of ice-cover simulated in our lake model is shown in dark blue. The average timing of ice-off dates and the timing of when lake ice-cover starts to form that is simulated in our lake model are shown in pale blue.

Formatted: Font: Bold, Not Italic

Formatted: Font: Not Italic

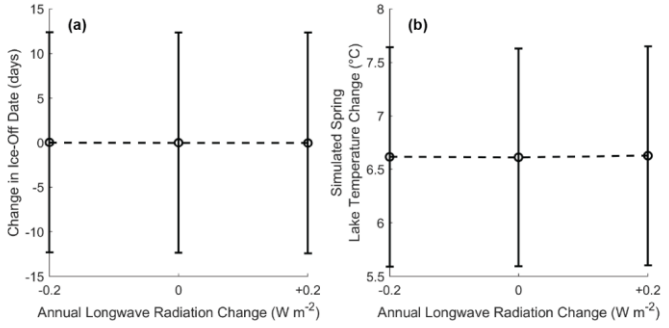

Figure A3. Lake model sensitivity tests showing the effect of annual longwave radiation perturbations on (a) ice-off dates and (b) lake water temperatures on May 1st.

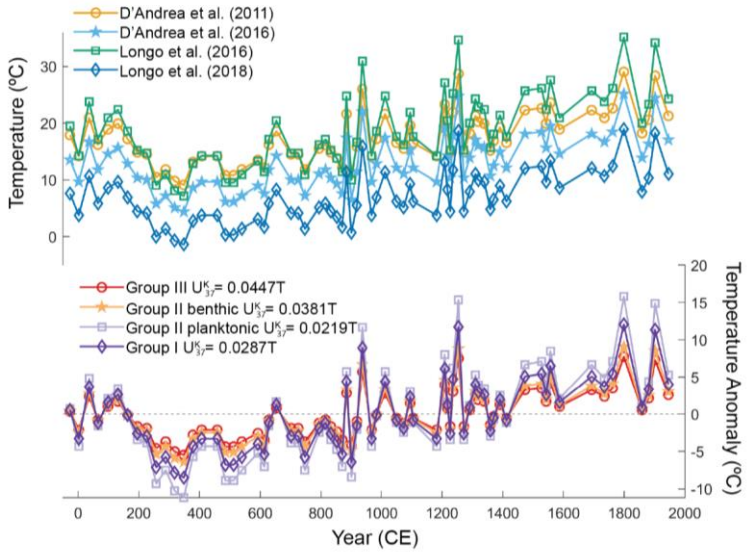

Figure A4. Alkenone calibrations from previous studies including (a) U^{K}_{37} = 0.0296T – 0.80 (D'Andrea et al., 2011), U^{K}_{37} = 0.0284T – 0.655 (D'Andrea et al., 2016), U^{K}_{37} = 0.021T – 0.68 (Longo et al., 2016), and U^{K}_{37} = 0.029T – 0.49 (Longo et al., 2018). (b) Temperature anomalies calculated from slopes previously determined by D'Andrea et al., (2016) for Group III, Group II benthic, Group II planktonic, and Group I.

~~Table A1. Lake energy balance model results for air temperature perturbations.~~

~~Temperature Perturbation~~	~~Ice-off Date (Julian Day)~~	~~Water Temperature on May 1st (°C)~~
~~Control 0 °C~~	~~106 ± 9~~	~~6.6 ± 1.0~~
~~DJF -7 °C~~	~~119 ± 5~~	~~3.9 ± 2.3~~
~~DJF -3 °C~~	~~112 ± 5~~	~~6.1 ± 1.2~~

Formatted: Font: Bold, Not Italic
Formatted: Font: Bold, Not Italic
Formatted: Font: Not Italic
Formatted: Font: Bold, Not Italic
Formatted: Font: Not Italic
Formatted: Font: Bold, Not Italic
Formatted: Font: Not Italic
Formatted: Font: Bold, Not Italic
Formatted: Font: Bold, Not Italic
Formatted: Font: Not Italic
Formatted: Font: Bold, Not Italic
Formatted: Font: Not Italic
Formatted: Font: Not Italic
Formatted: Font: Not Italic
Formatted: Font: Not Italic
Formatted: Font: Not Italic
Formatted: Font: Not Italic
Formatted: Font: Bold, Not Italic
Formatted: Font: Not Italic
Formatted: Font: Not Italic
Formatted: Font: Not Italic

~~**DJF +3 °C**~~	~~93 ± 24~~	~~6.9 ± 1.0~~
~~**DJF +7 °C**~~	~~83 ± 30~~	~~6.9 ± 1.0~~
~~**MAM -7 °C**~~	~~129 ± 6~~	~~1.6 ± 1.4~~
~~**MAM -3 °C**~~	~~118 ± 6~~	~~4.8 ± 1.9~~
~~**MAM +3 °C**~~	~~95 ± 8~~	~~7.9 ± 1.0~~
~~**MAM +7 °C**~~	~~87 ± 8~~	~~9.6 ± 1.0~~
~~**JJA -7 °C**~~	~~106 ± 9~~	~~6.6 ± 1.0~~
~~**JJA -3 °C**~~	~~106 ± 9~~	~~6.6 ± 1.0~~
~~**JJA +3 °C**~~	~~106 ± 9~~	~~6.6 ± 1.0~~
~~**JJA +7 °C**~~	~~106 ± 8~~	~~6.6 ± 1.0~~
~~**SON -7 °C**~~	~~109 ± 6~~	~~6.8 ± 1.0~~
~~**SON -3 °C**~~	~~107 ± 6~~	~~6.7 ± 1.0~~
~~**SON +3 °C**~~	~~105 ± 9~~	~~6.6 ± 1.0~~
~~**SON +7 °C**~~	~~105 ± 9~~	~~6.7 ± 1.0~~

Table A2. Lake energy balance model results for shortwave solar radiation perturbations.

Shortwave Solar Radiation Perturbation	Ice-off Date (Julian Day)	Water Temperature on May 1st (°C)
Control	105 ± 9	6.6 ± 1.0
DJF x 0.50	108 ± 8	6.5 ± 1.0
DJF x 0.25	107 ± 8	6.5 ± 1.0
DJF x 1.25	105 ± 9	6.7 ± 1.0
DJF x 1.50	104 ± 9	6.8 ± 1.0
MAM x 0.50	124 ± 8	1.8 ± 1.6
MAM x 0.25	112 ± 9	4.5 ± 1.6
MAM x 1.25	100 ± 8	8.2 ± 1.2
MAM x 1.50	95 ± 7	9.8 ± 1.3
JJA x 0.50	106 ± 9	6.6 ± 1.0
JJA x 0.25	106 ± 9	6.6 ± 1.0
JJA x 1.25	106 ± 9	6.6 ± 1.0
JJA x 1.50	106 ± 8	6.6 ± 1.0
SON x 0.50	106 ± 8	6.5 ± 1.0
SON x 0.25	106 ± 9	6.6 ± 1.0
SON x 1.25	106 ± 8	6.6 ± 1.0
SON x 1.50	105 ± 8	6.7 ± 1.0

680

Table A3. Lake energy balance model results for longwave radiation perturbations.

Longwave Radiation Perturbation	Ice-off Date (Julian Day)	Water Temperature on May 1st (°C)

Control	105 ± 9	6.6 ± 1.0
-0.2 W m^{-2}	105 ± 9	6.6 ± 1.0
+0.2 W m^{-2}	105 ± 9	6.6 ± 1.0

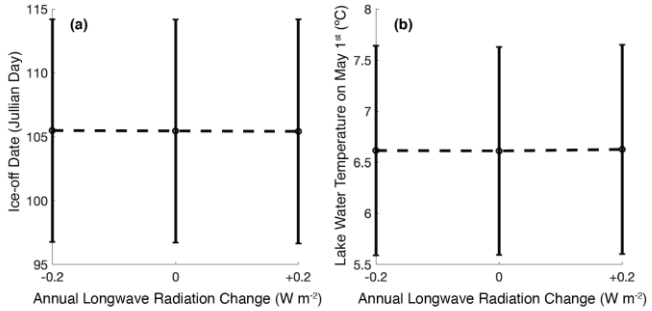

685 **Figure A1. Lake model sensitivity tests showing the effect of annual longwave radiation perturbations on (a) ice-off dates and (b) lake water temperatures on May 1st.**

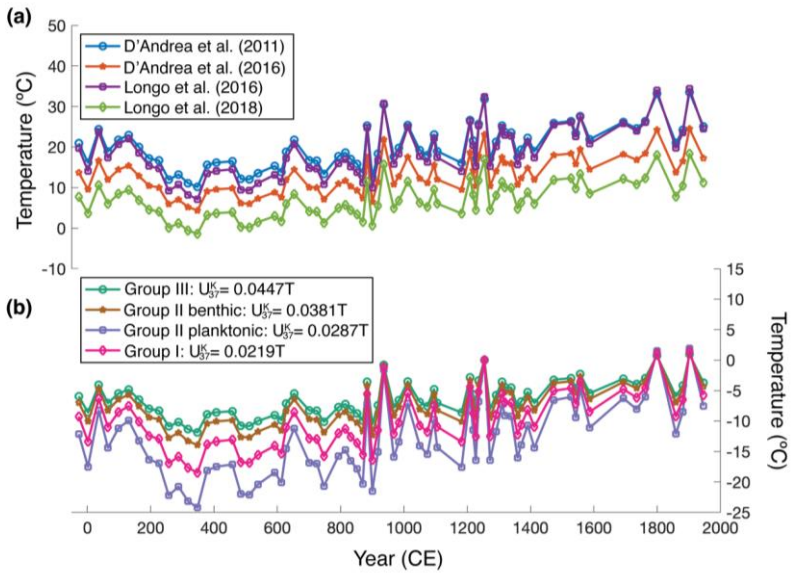

690 **Figure A2. Alkenone calibrations from previous studies including (a) D'Andrea et al., (2011), D'Andrea et al., (2016), Longo et al., (2016), Longo et al., (2018). (b) Different temperatures calculated from slopes previously determined by D'Andrea et al., (2016) for Group III, Group II benthic, Group II planktonic, and Group I.**

Data availability

Data will be made available at the National Oceanic and Atmospheric Administration National Centers for Environmental Information (NOAA NCEI) Paleoclimate Database: https://www.ncdc.noaa.gov/paleo/study/29992. The age model and information about the lake sediment core were obtained from Blair et al. (2015). Information about the lake energy balance model used in this study can be found in Dee et al. (2018) and the code for the lake energy balance model is available at: https://github.com/sylvia-dee/PRYSM. ERA-Interim daily data (1979-2019 CE) was obtained from: https://www.ecmwf.int/en/forecasts/datasets/reanalysis-datasets/era-interim (ECMWF; Dee et al., 2011). Meteorological data for southwest Iceland was obtained from: (https://en.vedur.is/climatology/data/; Icelandic Meteorological Office). Data used to make the maps in Fig. 1 can be found at: Natural Earth (https://www.naturalearthdata.com/), the National Land Survey of Iceland (https://www.lmi.is/en/), and the National Oceanic and Atmospheric Administration (NOAA) World Ocean Database (https://www.nodc.noaa.gov/OC5/WOD/pr_wod.html; Boyer et al., 2018~~in preparation~~). Satellite imagery for Table A3 was obtained from Planet Labs Inc. (https://www.planet.com/).

Author contributions

Study conceptualized by NR, JMR, and YH. Method development and laboratory analyses by NR and JG. NR prepared the manuscript with contributions from all co-authors.

Competing interests

The authors declare that they have no conflict of interest.

Acknowledgements

This project was funded by Geological Society of America Graduate Student Research Grants, the Nicole Rosenthal Hartnett Graduate Fellowship, Brown University Graduate School, and Brown University Undergraduate Teaching and Research Awards. We would like to thank Prof. T.D. Herbert, R. Rose, Dr. J. Salacup, Dr. G. Weiss, Dr. C. Morrill, A. Neary, Prof. S.G. Dee, and E. Kyzivat for advice and analytical support. All of the samples for this project were obtained from LacCore (National Lacustrine Core Facility), Department of Earth Sciences, University of Minnesota-Twin Cities. We would also like to thank the reviewers and David Harning for helping to improve this manuscript.

References

Adalsteinsson, H., Jónasson, P. M., & Rist, S.: Physical characteristics of Thingvallavatn, Iceland. Oikos, 121-135, https://doi.org/10.2307/3545048, 1992.

Andradóttir H.Ó.: Icelandic Lakes, Physical Characteristics. In: Bengtsson L., Herschy R.W., Fairbridge R.W. (eds) Encyclopedia of Lakes and Reservoirs. Encyclopedia of Earth Sciences Series. Springer, Dordrecht. https://doi.org/10.1007/978-1-4020-4410-6_224, 2012.

Assel, R. A. and Robertson, D. M.: Changes in winter air temperatures near Lake Michigan, 1851-1993, as determined from regional lake-ice records. Limnol. Oceanogr., 40, 165-176, https://doi.org/10.4319/lo.1995.40.1.0165, 1995.

Axford, Y., Geirsdóttir, A., Miller, G.H., and Langdon, P.G.: Climate of the Little Ice Age and the past 2000 years in northeast Iceland inferred from chironomids and other lake sediment proxies. J. Paleolimnol., 41, 7-24, https://doi.org/10.1007/s10933-008-9251-1, 2009.

Axford, Y., Andresen, C.S., Andrews, J.T., Belt, S.T., Geirsdóttir, Á., Massé, G., Miller, G.H., Ólafsdóttir, S. and Vare, L.L.: Do paleoclimate proxies agree? A test comparing 19 late Holocene climate and sea-ice reconstructions from Icelandic marine and lake sediments. J. Quat. Sci., 26, 645-656, https://doi.org/10.1002/jqs.1487, 2011.

Baker, J. L., Lachniet, M. S., Chervyatsova, O., Asmerom, Y., and Polyak, V. J.: Holocene warming in western continental Eurasia driven by glacial retreat and greenhouse forcing. Nat. Geosci., 10, 430-435, https://doi.org/10.1038/ngeo2953, 2017.

Berner, K. S., Koç, N., Divine, D., Godtliebsen, F., and Moros, M.: A decadal-scale Holocene sea surface temperature record from the subpolar North Atlantic constructed using diatoms and statistics and its relation to other climate parameters. Paleoceanography, 23, https://doi.org/10.1029/2006PA001339, 2008.

Blaauw, M.: Methods and code for 'classical' age-modelling of radiocarbon sequences. Quat. Geochronol., 5, 512-518, https://doi.org/10.1016/j.quageo.2010.01.002, 2010.

Blair, C. L., Geirsdóttir, Á., and Miller, G. H.: A high-resolution multi-proxy lake record of Holocene environmental change in southern Iceland. J. Quat. Sci., 30, 281-292, https://doi.org/10.1002/jqs.2780, 2015.

Boyer, T.P., Baranova, O. K., Coleman, C., Garcia, H. E., Grodsky, A., Locarnini, R. A., Mishonov, A. V., O'Brien, T.D., Paver, C.R., Reagan, J.R., Seidov, D., Smolyar, I. V., Weathers, K., and Zweng, M. M.: World Ocean Database 2018, (in preparation).

Brassell, S. C., Eglinton, G., Marlowe, I. T., Pflaumann, U., and Sarnthein, M.: Molecular stratigraphy: a new tool for climatic assessment. Nature, 320, 129, https://doi.org/10.1038/320129a0, 1986.

Cabedo-Sanz, P., Belt, S. T., Jennings, A. E., Andrews, J. T., and Geirsdóttir, Á.: Variability in drift ice export from the Arctic Ocean to the North Icelandic Shelf over the last 8000 years: a multi-proxy evaluation. Quat. Sci. Rev., 146, 99-115, https://doi.org/10.1016/j.quascirev.2016.06.012, 2016.

Formatted: Normal, Line spacing: single

Formatted: Condensed by 0.25 pt, Pattern: Clear (White)

Christensen, C. L.: Multi-proxy responses of Icelandic lakes to Holocene tephra perturbations (Doctoral dissertation, University of Colorado at Boulder), 2013.

Conte, M. H., Sicre, M. A., Rühlemann, C., Weber, J. C., Schulte, S., Schulz-Bull, D., and Blanz, T.: Global temperature calibration of the alkenone unsaturation index ($U^{K'}_{37}$) in surface waters and comparison with surface sediments. Geochem. Geophy. Geosy., 7, https://doi.org/10.1029/2005GC001054, 2006.

Coolen, M. J., Muyzer, G., Rijpstra, W. I. C., Schouten, S., Volkman, J. K., and Damsté, J. S. S.: Combined DNA and lipid analyses of sediments reveal changes in Holocene haptophyte and diatom populations in an Antarctic lake. Earth Planet. Sci. Lett., 223, 225-239, https://doi.org/10.1016/j.epsl.2004.04.014, 2004.

Cook, T. L., Bradley, R. S., Stoner, J. S., and Francus, P.: Five thousand years of sediment transfer in a high arctic watershed recorded in annually laminated sediments from Lower Murray Lake, Ellesmere Island, Nunavut, Canada. J. Paleolimnol., 41, 77, https://doi.org/10.1007/s10933-008-9252-0, 2009.

D'Andrea, W. J., and Huang, Y.: Long chain alkenones in Greenland lake sediments: Low $\delta^{13}C$ values and exceptional abundance. Org. Geochem., 36, 1234-1241, https://doi.org/10.1016/j.orggeochem.2005.05.001, 2005.

D'Andrea, W. J., Liu, Z., Alexandre, M. D. R., Wattley, S., Herbert, T. D., and Huang, Y.: An efficient method for isolating individual long-chain alkenones for compound-specific hydrogen isotope analysis. Anal. Chem., 79, 3430-3435, https://doi.org/10.1021/ac062067w, 2007.

D'Andrea, W. J., Huang, Y., Fritz, S. C., and Anderson, N. J.: Abrupt Holocene climate change as an important factor for human migration in West Greenland. Proc. Natl. Acad. Sci., 108, 9765-9769, https://doi.org/10.1073/pnas.1101708108, 2011.

D'Andrea, W. J., Vaillencourt, D. A., Balascio, N. L., Werner, A., Roof, S. R., Retelle, M., and Bradley, R. S.: Mild Little Ice Age and unprecedented recent warmth in an 1800 year lake sediment record from Svalbard. Geology, 40, 1007-1010, https://doi.org/10.1130/G33365.1, 2012.

D'Andrea, W. J., Theroux, S., Bradley, R. S., and Huang, X.: Does phylogeny control U^{K}_{37} -temperature sensitivity? Implications for lacustrine alkenone paleothermometry. Geochim. Cosmochim. Acta, 175, 168-180, https://doi.org/10.1016/j.gca.2015.10.031, 2016.

Dee, D. P., Uppala, S. M., Simmons, A. J., Berrisford, P., Poli, P., Kobayashi, S., Andrae, U., Balmaseda, M. A., Balsamo, G., Bauer, P., Bechtold, P., Beljaars, A. C. M., van de Berg, L., Bidlot, J., Bormann, N., Delsol, C., Dragani, R., Fuentes, M., Geer, A. J., Haimberger, L., Healy, S. B., Hersbach, H., Hólm, E. V., Isaksen, L., Kållberg, P., Köhler, M., Matricardi, M., McNally, A. P., Monge-Sanz, B. M., Morcrette, J. J., Park, B. K., Peubey, C., de Rosnay, P., Tavolato, C., Thépaut, J. N., and Vitart, F.: The ERA-Interim reanalysis: configuration and performance of the data assimilation system, Q. J. Roy. Meteor. Soc., 137, 553–597, https://doi.org/10.1002/qj.828, 2011.

Dee, S. G., Russell, J. M., Morrill, C., Chen, Z., and Neary, A.: PRYSM v2. 0: A Proxy System Model for Lacustrine Archives. Paleoceanogr. Paleocl., 33, 1250-1269, https://doi.org/10.1029/2018PA003413, 2018.

Formatted: Font: (Default) +Headings (Times New Roman)

Formatted: Font: (Default) +Headings (Times New Roman), Not Italic

Formatted: Font: (Default) +Headings (Times New Roman)

Delworth, T.L., Zeng, F., Vecchi, G.A., Yang, X., Zhang, L. and Zhang, R.: The North Atlantic Oscillation as a driver of rapid climate change in the Northern Hemisphere. Nature Geosci., 9, 509–512, https://doi.org/10.1038/ngeo2738, 2016.

Descy, J., Plisnier, P., Leporcq, B., Sténuite, S., Pirlot, S., Stimart, J., Gosselain, V., André, L., Alleman, L., Langlet, D., Descy, J.-P., Plisnier, P.-D., Leporcq, B., Sténuite, S., Pirlot, S., Stimart, J., Gosselain, V., André, L., Alleman, L., Langlet, D., Vyverman3, W., Cocquyt, C., De Wever, A., Stoyneva, M. P., Deleersnijder, E., Naithani4, J., Chitamwebwa5, D., Kimirei, A. C., Sekadende, B., Mwaitega, S., Muhoza5, S., Sinyenza, D., Makasa, L., Lukwessa, C., Zulu, I., & Phiri, H.: Climate variability as recorded in Lake Tanganyika (CLIMLAKE). Brussels: Belgian Science Policy, 2006.

Divine, D., Isaksson, E., Martma, T., Meijer, H.A., Moore, J., Pohjola, V., van de Wal, R.S., and Godtliebsen, F.: Thousand years of winter surface air temperature variations in Svalbard and northern Norway reconstructed from ice-core data. Polar Res., 30, 7379, https://doi.org/10.3402/polar.v30i0.7379, 2011a.

Divine, D.V., Sjolte, J., Isaksson, E., Meijer, H.A.J., Van De Wal, R.S.W., Martma, T., Pohjola, V., Sturm, C., and Godtliebsen, F.: Modelling the regional climate and isotopic composition of Svalbard precipitation using REMOiso: a comparison with available GNIP and ice core data. Hydrol. Process., 25, 3748-3759, https://doi.org/10.1002/hyp.8100, 2011b.

Eden, C. and Jung, T.: North Atlantic interdecadal variability: oceanic response to the North Atlantic Oscillation (1865–1997). J. Clim., 14, 676-691, https://doi.org/10.1175/1520-0442(2001)014<0676:NAIVOR>2.0.CO;2, 2001.

Einarsson, M. Á.: Climate of Iceland. World Survey of Climatology, 15, 673-697, 1984.

Gathorne-Hardy, F.J., Erlendsson, E., Langdon, P.G., and Edwards, K.J.: Lake sediment evidence for late Holocene climate change and landscape erosion in western Iceland. J. Paleolimnol., 42, 413-426, https://doi.org/10.1007/s10933-008-9285-4, 2009.

Geirsdóttir, Á., Miller, G.H., Thordarson, T., and Ólafsdóttir, K.B.: A 2000 year record of climate variations reconstructed from Haukadalsvatn, West Iceland. J. Paleolimnol., 41, 95-115, https://doi.org/10.1007/s10933-008-9253-z, 2009.

Geirsdóttir, Á., Miller, G.H., Andrews, J.T., Harning, D.J., Anderson, L.S., Florian, C., Larsen, D.J., and Thordarson, T.: The onset of Neoglaciation in Iceland and the 4.2 ka event. Clim. Past, 15, 25-40, https://doi.org/10.5194/cp-15-25-2019, 2019.

Haltia-Hovi, E., Saarinen, T., and Kukkonen, M.: A 2000-year record of solar forcing on varved lake sediment in eastern Finland. Quat. Sci. Rev., 26, 678-689, https://doi.org/10.1016/j.quascirev.2006.11.005, 2007.

Hanna, E., Jónsson, T., and Box, J. E.: An analysis of Icelandic climate since the nineteenth century. Int. J. Climatol.: J. Roy. Meteor. Soc., 24, 1193-1210, https://doi.org/10.1002/joc.1051, 2004.

Hanna, E., Jónsson, T., Ólafsson, J., and Valdimarsson, H.: Icelandic coastal sea surface temperature records constructed: putting the pulse on air–sea–climate interactions in the northern North Atlantic. Part I: comparison with HadISST1 open-ocean surface temperatures and preliminary analysis of long-term patterns and anomalies of SSTs around Iceland. J.Clim., 19, 5652-5666, https://doi.org/10.1175/JCLI3933.1, 2006.

Formatted: Font: (Default) Times New Roman

Formatted: Font: (Default) Times New Roman

Formatted: Font: (Default) Times New Roman, Not Italic

Formatted: Font: (Default) Times New Roman

Formatted: Font: (Default) Times New Roman, Not Italic

Formatted: Font: (Default) Times New Roman

Harning, D.J., Andrews, J.T., Belt, S.T., Cabedo-Sanz, P., Geirsdóttir, Á., Dildar, N., Miller, G.H. and Sepúlveda, J.: Sea Ice Control on Winter Subsurface Temperatures of the North Iceland Shelf During the Little Ice Age: A TEX_{86} Calibration Case Study. Paleoceanogr. Paleoclimatol., 34, 1006-1021, https://doi.org/10.1029/2018PA003523, 2019.

Harning, D. J., Curtin, L., Geirsdóttir, Á., D'Andrea, W. J., Miller, G. H., & Sepúlveda, J.: Lipid biomarkers quantify Holocene summer temperature and ice cap sensitivity in Icelandic lakes. Geophys. Res. Lett., 47, https://doi.org/10.1029/2019GL085728, 2020.

Helama, S., Jones, P. D., and Briffa, K. R.: Dark Ages Cold Period: A literature review and directions for future research. Holocene, 27, 1600-1606, https://doi.org/10.1177/0959683617693898, 2017.

Holmes, N., Langdon, P. G., Caseldine, C. J., Wastegård, S., Leng, M. J., Croudace, I. W., and Davies, S. M.: Climatic variability during the last millennium in Western Iceland from lake sediment records. Holocene, 26, 756-771, https://doi.org/10.1177/0959683615618260, 2016.

Hurrell, J.W.: Decadal trends in the North Atlantic Oscillation: regional temperatures and precipitation. Science, 269, 676-679, https://doi.org/10.1126/science.269.5224.676, 1995.

Icelandic Meteorological Office: https://en.vedur.is/climatology/data/, last access: 11 June 2020.

Isaksson, E., Divine, D., Kohler, J., Martma, T., Pohjola, V., Motoyama, H., and Watanabe, O.: Climate oscillations as recorded in Svalbard ice core $\omega^{18}O$ records between ad 1200 and 1997. Geogr. Ann. A., 87, 203-214, https://doi.org/10.1111/j.0435-3676.2005.00253.x, 2005.

Jiang, H., Eiríksson, J., Schulz, M., Knudsen, K.L., and Seidenkrantz, M.S.: Evidence for solar forcing of sea-surface temperature on the North Icelandic Shelf during the late Holocene. Geology, 33, 73-76, https://doi.org/10.1130/G21130.1, 2005.

Jiang, H., Muscheler, R., Björck, S., Seidenkrantz, M.S., Olsen, J., Sha, L., Sjolte, J., Eiríksson, J., Ran, L., Knudsen, K.L., and Knudsen, M.F.: Solar forcing of Holocene summer sea-surface temperatures in the northern North Atlantic. Geology, 43(3), 203-206, https://doi.org/10.1130/G36377.1, 2015.

Justwan, A., Koç, N., and Jennings, A.E.: Evolution of the Irminger and East Icelandic Current systems through the Holocene, revealed by diatom-based sea surface temperature reconstructions. Quat. Sci. Rev., 27, 1571-1582, https://doi.org/10.1016/j.quascirev.2008.05.006, 2008.

Kaufman, D. S., Schneider, D. P., McKay, N. P., Ammann, C. M., Bradley, R. S., Briffa, K. R., Miller, G.H., Otto-Bliesner, B.L., Overpeck, J.T., Vinther, B.M., and Lakes, A.: Recent warming reverses long-term Arctic cooling. Science, 325, 1236-1239, https://doi.org/10.1126/science.1173983, 2009.

Landl, B., Björnsson, H., & Kuhn, M.: The energy balance of calved ice in Lake Jökulsarlón, Iceland. Arct., Antarct., and Alp. Res., 35, 475-481, 2003.

Langdon, P.G., Caseldine, C.J., Croudace, I.W., Jarvis, S., Wastegård, S., and Crowford, T.C.: A chironomid-based reconstruction of summer temperatures in NW Iceland since AD 1650. Quat. Res., 75, 451-460, https://doi.org/10.1016/j.yqres.2010.11.007, 2011.

Larsen, G. and Eiríksson, J.: Late Quaternary terrestrial tephrochronology of Iceland—frequency of explosive eruptions, type and volume of tephra deposits. J. Quat. Sci., 23, 109–120, https://doi.org/10.1002/jqs.1129, 2008.

Larsen, D.J., Miller, G.H., Geirsdóttir, Á., and Thordarson, T.: A 3000-year varved record of glacier activity and climate change from the proglacial lake Hvítárvatn, Iceland. Quat. Sci. Rev., 30, 2715-2731, https://doi.org/10.1016/j.quascirev.2011.05.026, 2011.

Laskar, J., Robutel, P., Joutel, F., Gastineau, M., Correia, A. C. M., and Levrard, B.: A long-term numerical solution for the insolation quantities of the Earth. Astron. Astrophys., 428, 261-285, https://doi.org/10.1051/0004-6361:20041335, 2004.

Latif, M., Böning, C., Willebrand, J., Biastoch, A., Dengg, J., Keenlyside, N., Schweckendiek, U., and Madec, G.: Is the Thermohaline Circulation Changing?, J. Clim., 19, 4631-4637, https://doi.org/10.1175/JCLI3876.1, 2006.

Liu, Z., Zhu, J., Rosenthal, Y., Zhang, X., Otto-Bliesner, B.L., Timmermann, A., Smith, R.S., Lohmann, G., Zheng, W., and Timm, O.E.: The Holocene temperature conundrum. Proc. Natl. Acad. Sci., 111, E3501-E3505, https://doi.org/10.1073/pnas.1407229111, 2014.

Ljungqvist, F. C., Zhang, Q., Brattström, G., Krusic, P. J., Seim, A., Li, Q., Zhang, Q., and Moberg, A.: Centennial-Scale Temperature Change in Last Millennium Simulations and Proxy-Based Reconstructions, J Clim., 32, 2441-2482, https://doi.org/10.1175/JCLI-D-18-0525.1, 2019.

Longo, W. M., Theroux, S., Giblin, A. E., Zheng, Y., Dillon, J. T., and Huang, Y.: Temperature calibration and phylogenetically distinct distributions for freshwater alkenones: evidence from northern Alaskan lakes. Geochim. Cosmochim. Ac., 180, 177-196, https://doi.org/10.1016/j.gca.2016.02.019, 2016.

Longo, W.M., Huang, Y., Yao, Y., Zhao, J., Giblin, A.E., Wang, X., Zech, R., Haberzettl, T., Jardillier, L., Toney, J., and Liu, Z.: Widespread occurrence of distinct alkenones from Group I haptophytes in freshwater lakes: Implications for paleotemperature and paleoenvironmental reconstructions. Earth Planet. Sci. Lett., 492, 239-250, https://doi.org/10.1016/j.epsl.2018.04.002, 2018.

Longo, W. M., Huang, Y., Russell, J. M., Morrill, C., Daniels, W. C., Giblin, A. E., & Crowther, J.: Insolation and greenhouse gases drove Holocene winter and spring warming in Arctic Alaska. Quat.~~ernary~~ Sci.~~ence Reviews~~Rev., 242, 106438, https://doi.org/10.1016/j.quascirev.2020.106438, 2020.

Malmquist, H. J., Antonsson, Þ., Ingvason, H. R., Ingimarsson, F., & Arnason, F.: Salmonid fish and warming of shallow Lake Elliðavatn in Southwest Iceland. Internationale Vereinigung für theoretische und angewandte Limnologie: Verhandlungen, 30, 1127-1132, https://doi.org/10.1080/03680770.2009.11902317, 2009.

Mangini, A., Spötl, C., and Verdes, P.: Reconstruction of temperature in the Central Alps during the past 2000 yr from a $\delta^{18}O$ stalagmite record. Earth Planet. Sci. Lett., 235, 741-751, https://doi.org/10.1016/j.epsl.2005.05.010, 2005.

Marsicek, J., Shuman, B. N., Bartlein, P. J., Shafer, S. L., and Brewer, S.: Reconciling divergent trends and millennial variations in Holocene temperatures. Nature, 554, 92-96, https://doi.org/10.1038/nature25464, 2018.

Formatted: Dutch (Netherlands), Condensed by 0.25 pt, Pattern: Clear (White)

Massé, G., Rowland, S. J., Sicre, M. A., Jacob, J., Jansen, E., and Belt, S. T.: Abrupt climate changes for Iceland during the last millennium: evidence from high resolution sea ice reconstructions. Earth Planet. Sci. Lett., 269, 565-569, https://doi.org/10.1016/j.epsl.2008.03.017, 2008.

Mauri, A., Davis, B. A. S., Collins, P. M., and Kaplan, J. O.: The climate of Europe during the Holocene: a gridded pollen-based reconstruction and its multi-proxy evaluation. Quat. Sci. Rev., 112, 109-127, https://doi.org/10.1016/j.quascirev.2015.01.013, 2015.

McKay, N. P., and Kaufman, D. S.: An extended Arctic proxy temperature database for the past 2,000 years. Sci. Data, 1, 1-10, https://doi.org/10.1038/sdata.2014.26, 2014.

Meyer, H., Opel, T., Laepple, T., Dereviagin, A.Y., Hoffmann, K. and Werner, M.: Long-term winter warming trend in the Siberian Arctic during the mid- to late Holocene. Nature Geosci., 8, 122–125, https://doi.org/10.1038/ngeo2349, 2015.

Miettinen, A., Divine, D., Koç, N., Godtliebsen, F., and Hall, I.R.: Multicentennial variability of the sea surface temperature gradient across the subpolar North Atlantic over the last 2.8 kyr. J. Clim. 25, 4205-4219, https://doi.org/10.1175/JCLI-D-11-00581.1, 2012.

Miller, G.H., Geirsdóttir, Á., Zhong, Y., Larsen, D.J., Otto-Bliesner, B.L., Holland, M.M., Bailey, D.A., Refsnider, K.A., Lehman, S.J., Southon, J.R. and Anderson, C.: Abrupt onset of the Little Ice Age triggered by volcanism and sustained by sea-ice/ocean feedbacks. Geophys. Res. Lett., 39, https://doi.org/10.1029/2011GL050168, 2012.

Moffa-Sánchez, P., Born, A., Hall, I. R., Thornalley, D. J., and Barker, S.: Solar forcing of North Atlantic surface temperature and salinity over the past millennium. Nat. Geosci., 7, 275-278, https://doi.org/10.1038/ngeo2094, 2014.

Moffa-Sánchez, P. and Hall, I.R.: North Atlantic variability and its links to European climate over the last 3000 years. Nat. Commun., 8, 1726, https://doi.org/10.1038/s41467-017-01884-8, 2017.

Moreno-Chamarro, E., Zanchettin, D., Lohmann, K., Luterbacher, J., and Jungclaus, J.: H. Winter amplification of the European Little Ice Age cooling by the subpolar gyre. Sci. Rep., 7, 9981, https://doi.org/10.1038/s41598-017-07969-0, 2017.

Moros, M., Andrews, J. T., Eberl, D. D., and Jansen, E.: Holocene history of drift ice in the northern North Atlantic: Evidence for different spatial and temporal modes. Paleoceanography, 21, https://doi.org/10.1029/2005PA001214, 2006.

Müller, P. J., Kirst, G., Ruhland, G., Von Storch, I., and Rosell-Melé, A.: Calibration of the alkenone paleotemperature index $U^{K'}_{37}$ based on core-tops from the eastern South Atlantic and the global ocean (60° N-60° S). Geochim. Cosmochim. Ac., 62, 1757-1772, https://doi.org/10.1029/2005GC001054, 1998.

Nakamura, H., Sawada, K., Araie, H., Suzuki, I., and Shiraiwa, Y.: Long chain alkenes, alkenones and alkenoates produced by the haptophyte alga Chrysotila lamellosa CCMP1307 isolated from a salt marsh. Org. Geochem., 66, 90-97, https://doi.org/10.1016/j.orggeochem.2013.11.007, 2014.

National Land Survey of Iceland: https://www.lmi.is/en/, last access: 24 June 2020.

Natural Earth: https://www.naturalearthdata.com/, last access: 24 June 2020.

Ogilvie, A. E.: The past climate and sea-ice record from Iceland, Part 1: Data to AD 1780. Clim. Change, 6, 131-152, https://doi.org/10.1007/BF00144609, 1984.

Ogilvie, A.E.J.: Documentary evidence for changes in the climate of Iceland AD 1500 to 1800, in: Climate since AD 1500, edited by: Bradley, R.S. and Jones, P.D., Routledge, London and New York, 92–117, 1992.

Ogilvie, A. E. J.: Sea-ice conditions off the coasts of Iceland AD 1601–1850 with special reference to part of the Maunder Minimum period (1675–1715). AmS-Varia, 25, 9-12, 1996.

Ogilvie, A. E., Barlow, L. K., and Jennings, A. E.: North Atlantic climate c. AD 1000: Millennial reflections on the Viking discoveries of Iceland, Greenland and North America. Weather, 55, 34-45, https://doi.org/10.1002/j.1477-8696.2000.tb04028.x, 2000.

Ogilvie, A. E., and Jónsson, T.: "Little Ice Age" research: A perspective from Iceland. Clim. Change, 48, 9-52, https://doi.org/10.1007/978-94-017-3352-6_1, 2001.

Ojala, A. E., and Alenius, T.: 10,000 years of interannual sedimentation recorded in the Lake Nautajärvi (Finland) clastic–organic varves. Palaeogeogr., Palaeoclimatol., Palaeoecol., 219, 285-302, https://doi.org/10.1016/j.palaeo.2005.01.002, 2005.

Ólafsdóttir, S., Jennings, A. E., Geirsdóttir, Á., Andrews, J., and Miller, G. H.: Holocene variability of the North Atlantic Irminger current on the south-and northwest shelf of Iceland. Mar. Micropaleontol., 77, 101-118, https://doi.org/10.1016/j.marmicro.2010.08.002, 2010.

Ólafsson, J.: Physical characteristics of lake Mývatn and river Laxá. Oikos, 38-66, https://doi.org/10.2307/3544220, 1979.

Ono, M., Sawada, K., Shiraiwa, Y., and Kubota, M.: Changes in alkenone and alkenoate distributions during acclimatization to salinity change in Isochrysis galbana: Implication for alkenone-based paleosalinity and paleothermometry. Geochem. J., 46, 235-247, https://doi.org/10.2343/geochemj.2.0203, 2012.

Opel T., Laepple T., Meyer H., Dereviagin A.Y., and Wetterich S.: Northeast Siberian ice wedges confirm Arctic winter warming over the past two millennia. Holocene, 27, 1789-1796, https://doi.org/10.1177/0959683617702229, 2017.

Orme, L.C., Miettinen, A., Divine, D., Husum, K., Pearce, C., Van Nieuwenhove, N., Born, A., Mohan, R. and Seidenkrantz, M.S.: Subpolar North Atlantic sea surface temperature since 6 ka BP: Indications of anomalous ocean-atmosphere interactions at 4-2 ka BP. Quat. Sci. Rev., 194, 128-142, https://doi.org/10.1016/j.quascirev.2018.07.007, 2018.

Otto-Bliesner, B. L., Brady, E. C., Fasullo, J., Jahn, A., Landrum, L., Stevenson, S., Rosenbloom, N., Mai, A., and Strand, G.: Climate variability and change since 850 CE: An ensemble approach with the Community Earth System Model. B.Am. Meteorol. Soc., 97, 735-754, https://doi.org/10.1175/BAMS-D-14-00233.1, 2016.

PAGES 2K Consortium: Continental-scale temperature variability during the past two millennia. Nat. Geosci., 6, 339-346, https://doi.org/10.1038/ngeo1797, 2013.

PAGES 2K Consortium: Consistent multi-decadal variability in global temperature reconstructions and simulations over the Common Era. Nat. Geosci., 12, 643-649, https://doi.org/10.1038/s41561-019-0400-0, 2019.

Pla, S., and Catalan, J.: Chrysophyte cysts from lake sediments reveal the submillennial winter/spring climate variability in the northwestern Mediterranean region throughout the Holocene. Clim. Dyn., 24, 263-278, https://doi.org/10.1007/s00382-004-0482-1, 2005.

Planet Labs Inc.: https://www.planet.com/

Prahl, F. G., and Wakeham, S. G.: Calibration of unsaturation patterns in long-chain ketone compositions for palaeotemperature assessment. Nature, 330, 367, https://doi.org/10.1038/330367a0, 1987.

Prahl, F. G., Muehlhausen, L. A., and Zahnle, D. L.: Further evaluation of long-chain alkenones as indicators of paleoceanographic conditions. Geochim. Cosmochim. Ac., 52, 2303-2310, https://doi.org/10.1016/0016-7037(88)90132-9, 1998.

Ran, L., Jiang, H., Knudsen, K.L. and Eiríksson, J.: Diatom-based reconstruction of palaeoceanographic changes on the North Icelandic shelf during the last millennium. Palaeogeogr., Palaeoclimatol., Palaeoecol., 302, 109-119, https://doi.org/10.1016/j.palaeo.2010.02.001, 2011.

Rehfeld, K., Trachsel, M., Telford, R. J., and Laepple, T.: Assessing performance and seasonal bias of pollen-based climate reconstructions in a perfect model world. Clim. Past, 12, 2255-2270, https://doi.org/10.5194/cp-12-2255-2016, 2016.

Richter, N., Longo, W. M., George, S., Shipunova, A., Huang, Y., and Amaral-Zettler, L.: Phylogenetic diversity in freshwater-dwelling Isochrysidales haptophytes with implications for alkenone production. Geobiology, 17, 272-280, https://doi.org/10.1111/gbi.12330, 2019.

Richter, N., Russell, J.M., Garfinkel, J., and Huang, Y.: Impacts of Norse settlement on terrestrial and aquatic ecosystems in Southwest Iceland. J. Paleolimnol., 65, 255–269, https://doi.org/10.1007/s10933-020-00169-3, 2021.

Salacup, J. M., Farmer, J. R., Herbert, T. D., and Prell, W. L.: Alkenone Paleothermometry in Coastal Settings: Evaluating the Potential for Highly Resolved Time Series of Sea Surface Temperature. Paleoceanogr. Paleoclimatol., 34, 164-181, https://doi.org/10.1029/2018PA003416, 2019.

Schmidt, G. A., Jungclaus, J. H., Ammann, C. M., Bard, E., Braconnot, P. C. T. J. D. G., Crowley, T. J., Delaygue, G., Joos, F., Krivova, N.A., Muscheler, R., and Otto-Bliesner, B. L.: Climate forcing reconstructions for use in PMIP simulations of the last millennium (v1. 0). Geosci. Model Devel., 4, 33-45, https://doi.org/10.5194/gmd-4-33-2011, 2011.

Sicre, M.A., Jacob, J., Ezat, U., Rousse, S., Kissel, C., Yiou, P., Eiríksson, J., Knudsen, K.L., Jansen, E., and Turon, J.L.: Decadal variability of sea surface temperatures off North Iceland over the last 2000 years. Earth Planet. Sci. Lett., 268, 137-142, https://doi.org/10.1016/j.epsl.2008.01.011, 2008.

Sicre, M.A., Hall, I.R., Mignot, J., Khodri, M., Ezat, U., Truong, M.X., Eiríksson, J., and Knudsen, K.L.: Sea surface temperature variability in the subpolar Atlantic over the last two millennia. Paleoceanography, 26, https://doi.org/10.1029/2011PA002169, 2011.

Sigl, M., Winstrup, M., McConnell, J.R., Welten, K.C., Plunkett, G., Ludlow, F., Büntgen, U., Caffee, M., Chellman, N., Dahl-Jensen, D., and Fischer, H.: Timing and climate forcing of volcanic eruptions for the past 2,500 years. Nature, 523, 543-549, https://doi.org/10.1038/nature14565, 2015.

Formatted: Font: (Default) +Headings (Times New Roman)

Formatted: English (United States)

Formatted: Font: (Default) +Headings (Times New Roman)

Formatted: Font: (Default) +Headings (Times New Roman), Not Italic

Formatted: Font: Not Italic

Formatted: Font: (Default) +Headings (Times New Roman), Not Italic

Formatted: Font: Not Italic

Formatted: Font: (Default) +Headings (Times New Roman)

Formatted: Font: (Default) +Headings (Times New Roman), Not Bold

Formatted: Font: (Default) +Headings (Times New Roman)

Formatted: Font: (Default) +Headings (Times New Roman)

Field Code Changed

Formatted: Hyperlink, Font: (Default) +Headings (Times New Roman), Font color: Auto, Pattern: Clear

Formatted: Font: (Default) +Headings (Times New Roman)

Steinhilber, F., Beer, J., and Fröhlich, C.: Total solar irradiance during the Holocene. Geophys. Res. Lett., 36, https://doi.org/10.1029/2009GL040142, 2009.

Sun, Q., Chu, G., Liu, G., Li, S., and Wang, X.: Calibration of alkenone unsaturation index with growth temperature for a lacustrine species, Chrysotila lamellosa (Haptophyceae). Org. Geochem., 38, 1226-1234, https://doi.org/10.1016/j.orggeochem.2007.04.007, 2007.

Theroux, S., D'Andrea, W. J., Toney, J., Amaral-Zettler, L., and Huang, Y.: Phylogenetic diversity and evolutionary relatedness of alkenone-producing haptophyte algae in lakes: implications for continental paleotemperature Earth Planet. Sci. Lett., 300, 311-320, https://doi.org/10.1016/j.epsl.2010.10.009, 2010.

Thornalley, D., Elderfield, H. and McCave, I.: Holocene oscillations in temperature and salinity of the surface subpolar North Atlantic. Nature, 457, 711–714, https://doi.org/10.1038/nature07717, 2009.

Toney, J. L., Huang, Y., Fritz, S. C., Baker, P. A., Grimm, E., and Nyren, P.: Climatic and environmental controls on the occurrence and distributions of long chain alkenones in lakes of the interior United States. Geochim. Cosmochim. Ac., 74, 1563-1578, https://doi.org/10.1016/j.gca.2009.11.021, 2010.

Toney, J. L., Theroux, S., Andersen, R. A., Coleman, A., Amaral-Zettler, L., and Huang, Y.: Culturing of the first 37: 4 predominant lacustrine haptophyte: geochemical, biochemical, and genetic implications. Geochim. Cosmochim. Ac., 78, 51-64, https://doi.org/10.1016/j.gca.2011.11.024, 2012.

van der Bilt, W. G., D'Andrea, W. J., Bakke, J., Balascio, N. L., Werner, J. P., Gjerde, M., and Bradley, R. S.: Alkenone-based reconstructions reveal four-phase Holocene temperature evolution for High Arctic Svalbard. Quat. Sci. Rev., 183, 204-213, https://doi.org/10.1016/j.quascirev.2016.10.006, 2018.

van der Bilt, W. G., D'Andrea, W. J., Werner, J. P., and Bakke, J.: Early Holocene temperature oscillations exceed amplitude of observed and projected warming in Svalbard lakes. Geophys. Res. Lett., 46, 14732-14741, https://doi.org/10.1029/2019GL084384, 2019.

Van Nieuwenhove, N., Pearce, C., Knudsen, M. F., Røy, H., and Seidenkrantz, M. S.: Meltwater and seasonality influence on subpolar Gyre circulation during the Holocene. Palaeogeogr., Palaeoclimatol., Palaeoecol., 502, 104-118, https://doi.org/10.1016/j.palaeo.2018.05.002, 2018.

Visbeck, M., Chassignet, E. P., Curry, R. G., Delworth, T. L., Dickson, R. R., and Krahmann, G.: The ocean's response to North Atlantic Oscillation variability. Geophys. Monogr. Sr., 134, 113-146, https://doi.org/10.1029/134GM06, 2003.

Wang, Z., and Liu, W.: Calibration of the $U^{K'}_{37}$ index of long-chain alkenones with the in-situ water temperature in Lake Qinghai in the Tibetan Plateau. Chinese Sci. Bull., 58, 803-808, https://doi.org/10.1007/s11434-012-5527-y, 2013.

Yao, Y., Zhao, J., Longo, W.M., Li, G., Wang, X., Vachula, R.S., Wang, K.J. and Huang, Y.: New insights into environmental controls on the occurrence and abundance of Group I alkenones and their paleoclimate applications: Evidence from volcanic lakes of northeastern China. Earth Planet. Sci. Lett., 527, https://doi.org/10.1016/j.epsl.2019.115792, 2019.

Yeager, S. G., and Robson, J. I.: Recent progress in understanding and predicting Atlantic decadal climate variability. Curr. Clim. Change Rep., 3, 112-127, https://doi.org/10.1007/s40641-017-0064-z, 2017.

Formatted: Font: (Default) Times New Roman

Formatted: Font: (Default) Times New Roman, English (United States)

Formatted: Font: (Default) Times New Roman

Formatted: Font: (Default) Times New Roman, Not Italic

Formatted: Font: (Default) Times New Roman

Formatted: Font: (Default) Times New Roman, Not Italic

Formatted: Font: (Default) Times New Roman

Formatted: Default Paragraph Font, Font: (Default) Times New Roman, 10 pt, Font color: Auto

Formatted: Font: (Default) Times New Roman

Formatted: Font: (Default) Times New Roman

Formatted: Font: (Default) Times New Roman, English (United States)

Formatted: Font: (Default) Times New Roman

Formatted: Font: (Default) Times New Roman, Not Italic

Formatted: Font: (Default) Times New Roman

Formatted: Font: (Default) Times New Roman, Not Italic

Formatted: Font: (Default) Times New Roman

Formatted: Default Paragraph Font, Font: (Default) Times New Roman, 10 pt, Not Bold, Font color: Auto, Pattern: Clear

Zheng, Y., Huang, Y., Andersen, R. A., and Amaral-Zettler, L. A.: Excluding the di-unsaturated alkenone in the U^{K}_{37} index strengthens temperature correlation for the common lacustrine and brackish-water haptophytes. Geochim. Cosmochim. Ac., 175, 36-46, https://doi.org/10.1016/j.gca.2015.11.024, 2016.

Zink, K. G., Leythaeuser, D., Melkonian, M., and Schwark, L.: Temperature dependency of long-chain alkenone distributions in recent to fossil limnic sediments and in lake waters. Geochim. Cosmochim. Ac., 65, 253-265, https://doi.org/10.1016/S0016-7037(00)00509-3, 2001.

Formatted: Normal, Indent: Left: 0 cm, Hanging: 0.63 cm